UNIVERSIDADE DA BEIRA INTERIOR
Ciências

Regulation of Aß-scavengers in the choroid plexus of Alzheimer´s disease patients.

André Pedro Oliveira

Dissertação para obtenção do Grau de Mestre em
Bioquímica
(2º ciclo de estudos)

Orientador: Prof. Dra. Cecília Santos
Coorientadoras: Dra. Joana Figueiró Silva e Dra. Eva Carro, Instituto de Investigación Hospital 12 de Octubre, Madrid

Covilhã, Junho de 2016

Acknowledgments

I would like to thank all the people involved in the course of this work, Prof. Cecilia Santos for the opportunity to study abroad, Eva Carro for her hospitality, and also thanks to the Neuroscience group of Instituto de Investigación 12 de Octubre.

A special thanks addressed to Joana Figueiró, a person that was always present since the very beginning of this work, for her personableness, support, advice, endless patience, for never doubting my capacities and, more importantly, for teaching me everything I put on this work. A person whose door was always open whenever I ran into a trouble spot or had a question about my work. Her willingness to give her time so generously has been very much appreciated. This dissertation is dedicated to her. Thank you Joanita.

Finally, I must express my very profound gratitude to my parents for providing me with unfailing support and continuous encouragement throughout my years of study and through the process of researching and writing this thesis. This accomplishment would not have been possible without them. Thank you.

Abstract

Alzheimer's disease (AD) is a neurodegenerative disorder described as a progressive cognitive impairment and represents the most frequent cause of dementia in the elderly. AD is considered to be a multifactorial disease, which is characterized by accumulation of extracellular amyloid-ß peptide (Aß) into soluble plaques in the brain, associated with the aggregation of tau protein into intracellular neurofibrillary tangles leading to neuronal loss. Recently, it has been demonstrated that the choroid plexus (CP) has a role counteracting in the disease progression, specifically, by producing Aß-scavengers and performing Aß clearance. Insulin-degrading enzyme (IDE), angiotensin-converting enzyme (ACE), gelsolin (GLS), neprilysin (NEP), transthyretin (TTR) and metallothionein-2A (MT2A), are categorized Aß-scavengers and perform the Aß clearance. Memory formation and cognitive functions are deeply influenced by sleep which is controlled by the circadian clock. The circadian rhythm comprises the human internal clock system, characterized by the suprachiasmatic nucleus (SCN). SCN represents the core of the circadian system, responsible for oscillations with a periodicity of approximately 24h in sleep-wake cycle, body temperature, feeding, rest-activity behavior, hormonal levels, among others. The regulation of the circadian rhythms depends on a set of clock genes, including circadian locomoter output cycles kaput (CLOCK), brain and muscle Arnt-like protein-1 (BMAL1) or aryl hydrocarbon receptor nuclear translocator-like (ARNTL), three PERIOD genes (PER1, PER2, and PER3) and two plant CRYPTOCHROME gene homologues (CRY1 and CRY2). During sleep there is an increase of Aß clearance in brain and also in CSF of healthy individuals, which contrasts with the diminished Aß clearance in AD brains. The hypothesis of this work study is that the circadian rhythm regulates the expression of Aß-scavengers in the CP of AD patients. Firstly, primers were designed for IDE, NEP, ACE, GLS, TTR, MT2A, CLOCK, BMAL1, PER2, PER3 and CRY2 genes, and respectively optimizations of their RT-qPCR reactions were also carried out with success. Finally, an analysis of mRNA expression levels of TTR, GLS and NEP genes was performed on the CP of AD patients along the stages of the disease by real-time quantitative PCR (RT-qPCR). TTR and GLS mRNA levels were significantly upregulated in Braak stage II, when compared to age-matched controls. In the following Braak stages, the levels returned normal levels as observed in age-matched controls. NEP mRNA levels displayed the same tendency but it did not reach statistical significance.

Keywords

Choroid plexus, circadian rhythm, Aß-scavengers, amyloid ß, Insulin-degrading enzyme, angiotensin-converting enzyme, gelsolin, neprilysin, transthyretin, metallothionein-2A, clock genes, Alzheimer´s disease

Resumo alargado

A doença de Alzheimer (DA) é uma doença neurodegenerativa descrita como um declínio cognitivo progressivo e representa a causa mais comum de demência na faixa etária mais avançada. A DA é considerada como uma doença multifatorial, caracterizada pela acumulação excessiva do péptido ß-amilóide (Aß) extracelular em placas solúveis em várias regiões do cérebro, associado com a agregação da proteína tau em emaranhados neurofibrilares intracelulares que levam a uma significativa perda neuronal. A acumulação de Aß é considerado o processo mais patogénico da doença. Este é gerado pela clivagem da proteína precursora amilóide (PPA) pelas ß- e γ-secretases que podem gerar três principais isoformas distintas: Aß 1-38, Aß 1-40 e Aß 1-42. A isoforma Aß 1-40 representa a mais solúvel e a Aß 1-42 a mais neurotóxica e mais propensa a agregar-se. Recentemente, foi demonstrado que o plexo coroide (PC) desempenha um papel importante na progressão da doença. O PC é uma estrutura altamente vascularizada localizada nos ventrículos cerebrais. Está envolvida numa panóplia de funções no cérebro, incluindo a secreção de líquido cefalorraquidiano, síntese e secreção de numerosas substâncias bioativas, algumas delas direta- ou indiretamente envolvidas na eliminação do péptido Aß. Este processo envolve proteínas e enzimas que são capazes de metabolizar e/ou eliminar o péptido no cérebro (*Aß-scavengers*), diminuindo assim a sua quantidade. Dentro das numerosas substancias bioativas secretadas pelo PC, destacam-se algumas que são relevantes para a eliminação de Aß do cérebro. Neste grupo incluem-se a enzima degradadora de insulina (EDI), a enzima conversora de angiotensina (ECA), a gelsolina (GLS), a neprilisina (NEP), a transtiretina (TTR) e a metalotioneína-2A (MT2A). Todas estas proteínas interagem com o péptido Aß, por mecanismos distintos, podendo encontrar-se sobre- ou sub-expressas no cérebro devido à doença de Alzheimer.

Uma das patologias mais comuns da doença de Alzheimer são as perturbações no sono e no ritmo circadiano, ambos bastante relacionados. O ritmo circadiano é estabelecido por um sistema relógio interno, que é um componente fundamental da fisiologia dos mamíferos, localizado no núcleo supraquiasmático (NSQ). O NSQ representa o centro do ritmo circadiano, responsável por oscilações com uma periodicidade de, aproximadamente, 24 h no ciclo dormir-acordar, manutenção da temperatura corporal, fome, comportamento repouso-atividade, níveis hormonais, entre outros. A regulação dos ritmos circadianos encontra-se sob a responsabilidade de um conjunto de genes relógio, incluindo *circadian locomotor output cycles kaput* (CLOCK), proteína-1 tipo-Arnt de cérebro e músculo (BMAL1), três genes PERIOD (PER1, PER2 e PER3) e dois genes homólogos CRYPTOCHROME (CRY1 e CRY2). Estes genes são capazes de controlar aproximadamente 10% de todos os genes expressos e podem ser considerados ubíquos. Quase todos os tecidos periféricos, incluindo regiões do cérebro fora do NSQ, contêm relógios circadianos autónomos, incluindo o PC. O mau funcionamento do relógio circadiano possui uma grande influência nos ciclos de sono/vigília e pensa-se que é capaz de

gerar mudanças que influenciam a formação de memórias e funções cognitivas. Durante a fase do sono existe um aumento da eliminação do péptido Aß no cérebro e também no líquido cefalorraquidiano de indivíduos saudáveis, o que contrasta com o baixo poder de eliminação de Aß no cérebro de pacientes com DA.

O objetivo deste estudo é verificar se a expressão de *Aß-scavengers* sofre alterações em plexos coroide de pacientes com DA por PCR quantitativa em tempo real e optmizar as condições de reação de PCR quantitativa em tempo real para os genes do ritmo circadiano com vista a proceder à sua análise também no PC de doentes com AD. Os pacientes foram divididos entre os estágios de Braak (I-VI) que são utilizados para caracterizar o estágio da doença pela quantidade e localização dos emaranhados neurofibrilares da proteína tau no cérebro de um individuo com DA.

A hipótese colocada neste trabalho seria verificar o ritmo circadiano dos *Aß-scavengers* no PC de pacientes com DA. Em primeiro lugar, foram desenhados primers para os genes IDE, NEP, ACE, GLS, TTR MT2A, CLOCK, BMAL1, PER2, PER3 e CRY2 usando um programa específico (PrimerBlast), seguindo os melhores ideais de termodinâmica. As otimizações da reação dos genes para RT-qPCR com vista a obter os melhores valores de eficiência e especificidade, foram realizadas com sucesso. Depois, foi realizada uma análise de expressão dos níveis de mRNA dos genes TTR, GLS e NEP ao longo dos estágios da doença por PCR quantitativa em tempo-real (RT-qPCR). Os resultados indicam uma sobre-regulaçao significativa dos niveis de mRNA de TTR e GLS no estágio II de Braak, em comparação com o grupo de controlo [TTR ($p< 0.0001$), GLS ($p< 0.01$). O mRNA do gene NEP não apresentou significância estatística nos seus níveis de expressão, apesar de se observar um ligeiro aumento da sua expressão nos estágio de Braak II, III e IV/V. Os genes TTR e GLS demonstraram diferenças significativas nos seus níveis de expressão em comparação com os restantes estágios de Braak, indicando uma sobre-regulação maioritária no estágio II de Braak, seguidos por uma sub-regulação da sua expressão nos estágios seguintes. Mais resultados são necessários para que seja possível verificar a existência de um padrão de regulação dos genes *Aß-scavengers*. Para uma futura análise da expressão génica dos genes do ritmo circadiano seria necessário aumentar o número de pacientes com DA com uma maior correspondência do número de horas de morte/recolha dos plexos coroide nos diferentes estágios da doença.

Palavras-chave

Plexos coroide, ritmo circadiano, Aß-scavengers, ß amilóide, enzima degradadora de insulina, enzima conversora de angiotensina, gelsolina, neprilisina, transtiretina, metalotioneína-2A, genes relógio, doença de Alzheimer

INDEX

I. INTRODUCTION

1. Alzheimer´s disease

Alzheimer's disease (AD) is a neurodegenerative disorder described as a progressive cognitive impairment, and is a current and emergent public health crisis with only a few number of effective treatments available (Lucey et al., 2014). It is considered the most frequent cause of dementia in the elderly (Urrestarazu et al., 2016).

1.1. Pathology and risk factors

The main pathological change in AD consist of brain atrophy, most significantly in the hippocampal formation, temporal lobes and parietotemporal cortices, accompanied by cortical thinning, enlarged ventricles, and white matter abnormalities (Tarasoff-Conway et al., 2015). The major early step in the pathogenesis of AD is the deposition of extracellular amyloid-ß peptide (Aß) into insoluble plaques in the brain, also associated with the aggregation of tau protein into intracellular neurofibrillary tangles leading to neuronal loss, synaptic dysfunction and cognitive impairment. (Hardy et al., 2002; Jack et al., 2010; Lucey et al., 2014). Accumulation of amyloid-ß peptide (Aß) into parenchymal senile plaques (also known as neuritic plaques) or in the walls of cerebral capillaries and arteries (known as cerebral amyloid angiopathy), aggregation of hyperphosphorylated tau into intracellular neurofibrillary tangles (NFTs) and neuropils threads are all microscopic alterations described in AD pathology (Tarasoff-Conway et al., 2015).

One of the most reported abnormalities in AD is circadian rhythm disruption, which affects more than 80% of AD patients over 65 years and include disturbances in sleep-wake cycles and thermoregulation (Van Someren, 2000; Song et al., 2015).

AD includes two main types of the disease, early-onset AD (EOAD) and sporadic or late-onset AD (LOAD). EOAD represents a minority of AD patients, while LOAD goes up to over 95% of patients with AD (Tarasoff-Conway et al., 2015).

When characterized by autosomal dominant inheritance, EOAD is associated with mutations in the presenilin 1 (*PSEN1*), presenilin 2 (*PSEN2*) or amyloid precursor protein (*APP*) genes.

The main overall risk factor for LOAD is ageing, although the evolution of cognitive impairment comes from genetics variants in the apolipoprotein E (APOE) ε4 allele. Environmental risk factors for LOAD, include cardiovascular disease and factors providing a risk of cardiovascular disease, such as diabetes mellitus and hypertension; head trauma and mental inactivity, and sleep impairment (Tarasoff-Conway et al., 2015).

The amyloid cascade theory proposes that Aß is central to the pathogenesis of AD. In this concept, either over-production or decreased clearance of Aß, will result in the formation of protofibrillar oligomers of Aß that aggregate and deposit as plaques. The deposition of

plaques causes the activation of microglia and astrocytes and all together can cause synaptic and neuritic injury. Then dementia is followed as a consequence of neuronal injury (Hirko, Meyer et al. 2007). However, there are other pathological mechanisms in this cascade involving neurotoxic effects of amyloid peptides probably producing oxidative damage and apoptosis in brain cells, including CP epithelial cells (Perez-Garcia et al., 2009; Vargas et al., 2010; Krzyzanowska et al., 2012).

1.2. Clinical stages of AD

AD can be clinically divided in three distinct phases: i) the pre-symptomatic or preclinical phase, ii) the symptomatic predementia phase, often referred to as mild cognitive impairment (MCI), and iii) the dementia phase. The MCI applies to patients who have some evidence of cognitive impairment but have not progressed to dementia (Sperling and Johnson, 2013).

Braak and Braak, 1991 proposed a neuropathological staging to differentiate initial, intermediate, and advanced AD based on the spread of neurofibrillary tangles (NFTs) within the medial temporal lobe memory circuit. Braak stage 0 corresponds to absence of NFTs, stages I-II (or transentohinal stages) to entorhinal-perirhinal cortex NFTs, stages III-IV (or limbic stages) to NFTs additionally in hippocampus and stages V-VI (or isocortical stages) to NFTs distributed in wider neocortical areas. Stages I-II represent clinically silent periods of the disease, the preclinical phase. Stages III-VI corresponds to clinically incipient AD, and stages V-VI correspond to fully developed AD (Braak and Braak, 1991; Mufson et al., 2016).

2. Amyloid-ß processing in AD

2.1. Aß peptide formation

The Aß peptide is mostly formed in the brain by neurons upon the cleavage of the amyloid precursor protein (APP) by ß- and γ-secretases (Figure 1) in the endoplasmic reticulum, Golgi apparatus, and endosomal-lysosomal pathway (Gonzalez-Marrero et al., 2015). It is cleaved into numerous isoforms of different amino acid lengths (Strooper et al., 2010; Lucey and Bateman 2014). The C-terminus of Aß plays a key role in amyloid aggregation (Chauhan et al., 1999). To be more exact, γ-secretase cuts the C-terminal end of the Aß peptide followed by cleavage of ß-secretase to produce 3 major isoforms, which are $Aß_{1-38}$, $Aß_{1-40}$ and $Aß_{1-42}$. The Aß isoforms are formerly secreted into the interstitial fluid (ISF; Cirrito et al., 2005; Lucey

and Bateman, 2014) and were identified in amyloid deposits in AD brain (Chauhan et al., 1999). On the contrary, if α-secretase cleaves APP inside the Aß domain, it prevents the formation of Aß in normal APP metabolism (Gonzalez-Marrero et al., 2015).

The Aß peptide exists in solution in a monomeric α-helical conformation. Aß fibril formation is a multi-step process which is headed by oligomerization and aggregation of Aß, and comprises conformational change of the peptide from α-helical to cross ß-pleated sheet secondary conformation (Ray et al., 2000). The Aß circulates in biological fluids at low nanomolar levels in a soluble form. $Aß_{1-40}$ is considered to be one of the major species of soluble Aß in body fluids and $Aß_{1-42}$, in turn is the main component of brain fibrillar deposits (Pérez et al., 2000). The $Aß_{1-40}$ is produced at higher concentrations while $Aß_{1-42}$ is more likely to aggregate due to its hydrophobic features, and is more neurotoxic (Jarrett et al., 1993; Pérez et al., 2000; Lucey and Bateman, 2014). $Aß_{1-42}$ neurotoxicity is correlated to its higher ß-sheet structure in comparison to $Aß_{1-40}$, being $Aß_{1-42}$ more fibrillogenic and cytotoxic than shorter Aßs. The peptide can be detectable in the cerebrospinal fluid (CSF) and plasma of normal individuals and patients with AD (Chauhan et al., 1999). Both neuritic and diffuse plaques contain predominantly $Aß_{1-42}$ and the cerebrovascular amyloid contains predominantly $Aß_{1-40}$. In the Aß soluble form it binds to several circulatory proteins, which will prevent Aß fibrillization or, alternatively, promote its polymerization (Qiao et al., 2004).

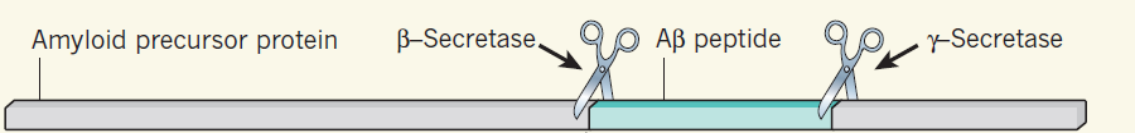

Figure 1 - The amyloid precursor protein (APP) is cleaved by the enzymes ß-secretase and γ-secretase into amyloid-ß (Aß) peptides (scissor symbols represent the cleavage sites; adapted from Peter et al., 2012).

2.2. Aß clearance in the brain

There are various pathways for the elimination of unwanted proteins in the brain, proteasomal and lysosomal degradation stand out as the major ones. Cells deploy numerous constitutive and regulated proteolytic activities that maintain proteostasis, all of them to work on regulating the biogenesis, trafficking, and degradation of proteins to maintain their steady-state levels. Evidences suggest that deficient clearance of Aß rather than increased production of the peptide contributes to its accumulation in LOAD (Baranello et al., 2015). In healthy individuals, the production and clearance are both fast, being the clearance slightly fast than the production, approximately 7,6% and 8,3%,respectively, of the total volume of Aß produced per hour. With this information it is possible to note that even a minor change in the production or clearance of Aß would soon cause anomalous accumulation in AD (Miners et

al., 2014). Despite the fact that only a few proteolytic pathways have been associated with degradation of Aß, there are quite a few enzymes with a wide specificity that seems to degrade Aß (Baranello et al., 2015).

Clearance through the blood-brain barrier (BBB) is suggested as the main pathway of Aß clearance, where Aß is removed across the BBB via transcytosis into the vascular lumen. This mechanism is thought to involve several transporter proteins and cell-surface receptors. Proteolytic degradation of Aß is considered the second most important pathway for Aß removal (Bohm et al., 2015). Proteolytic cleavage *in vitro* of the Aß generates fragments less neurotoxic and less prone to aggregation, and therefore, predicted peptide to be more easily cleared from the brain (Miners et al., 2014). The ability of the monomeric Aß peptide to assemble into soluble oligomers and then into more stable fibrils due to its tendency to aggregate is considered to be the third in the list of important pathways of Aß clearance (Bohm et al., 2015). Interestingly, experiments from large post-mortem human brain and *in vitro* studies have shown that the level and activity of many Aß-degrading proteases are increased in post-mortem brain tissue and upregulated by Aß which proposes the idea that the increases are secondary to Aß accumulation, probably demonstrating physiological responses to the rise in concentration of the Aß peptide (Miners et al., 2014). It is common sense that a healthy lifestyle enhances quality of life of the individual, and exercise has been demonstrated to benefit Aß clearance in mouse models of AD. Furthermore, physical activity showed to be linked with delayed Aß deposition in preclinical AD, whereas cognitively normal sedentary AD mouse models appeared to have an increased risk for cerebral amyloid deposition (Gallina et al., 2015).

In the last decade and half, several studies focused on possible aberrations of Aß clearance in late-onset sporadic AD, and described age- and disease-associated disruptions in the many clearance pathways, such as reductions in Aß-degrading protease activities (Miners et al., 2014). Along with aging, Aß aggregates become extremely difficult to be eliminated compared to soluble types, which explains why they are only visible many years previously to the beginning of other pathogenic events (Gallina et al., 2015). The rare autosomal dominant familial AD is mainly due to an overproduction of Aß, or promoting Aß protofibril formation, on the other hand, the late-onset sporadic AD is more common and is highly probable to be caused, in part, by diminished clearance of the Aß peptide from the CNS. Therefore, the deregulation of Aß clearance pathways in brain and at choroid plexus - cerebrospinal fluid (CP-CSF) seems to be a central disease event in some AD cases (Gonzalez-Marrero et al., 2015).

There is a group of proteins named Aß-scavengers, which can be produced by CP, characterized for being able to degrade and/or eliminate the Aß peptide from several brain regions in which they play a crucial role in the prevention of AD pathology (Carro et al., 2002; Zlokovic, 2004; Vargas et al., 2010).

2.2.1. Aß-scavengers

These proteins mainly comprise the Aß-degrading protease activity group. These Aß-scavengers include insulin-degrading enzyme, neprilysin, angiotensin-converting enzyme, gelsolin, transthyretin and metallothioneins (Chauhuan et al., 1999; Manso et al., 2011; Jochemsen et al., 2015; Alshehri et al., 2015; Hubin et al. 2016;).

2.2.1.1. Insulin-degrading enzyme

Insulin degrading enzyme (IDE) is a 110 kD zinc-dependent metallopeptidase which can be located in the peroxisomes, cytosol, and at the cell surface; it was also detected in human CSF. IDE is able to cleave a variety of small peptides, including insulin, glucagon, and insulin-like growth factors I and II, and this enzyme also converts ß-endorphin to γ-endorphin (Pérez et al., 2000; Baranello et al., 2015; Kochkina et al., 2015; Tang, 2016;). This enzyme is expressed in all tissues, and its levels can be controlled by various signals such as cellular stress, glucagon and free fatty acids (Tang, 2016).

Insulin-degrading enzyme (IDE), along with neprilysin (NEP), are considered to be the primary Aß-cleaving enzymes (Hubin et al., 2016). IDE is capable of cleaving Aß intra- and extracellularly and may prove valuable as a target to upregulate Aß clearance in impaired AD patients (Baranello et al., 2015). In addition, IDE actively regulates extracellular levels of Aß and has been reported to be proficient in degrading monomeric Aß, although, on the other hand there are few studies regarding IDE effect on Aß aggregates such as oligomers, and fibrils. In a more specific manner, reports have shown that IDE is capable of degrading $Aß_{1-40}$ into fragments that do not form aggregates upon prolonged incubation and to equally cleave $Aß_{1-42}$ and inhibit the formation of oligomers when acts in an early aggregation formation process of the oligomers, although IDE effect on $Aß_{1-42}$ is lower when compared to $Aß_{1-40}$ which reflects the higher aggregation propensity of $Aß_{1-42}$. Further experiments demonstrated that IDE exclusively degrades monomeric Aß due to its small catalytic chamber in comparison with the oligomeric and fibrillar forms of Aß which are too large to fit in the chamber itself. Regarding this data, IDE presence appears to induce a disruption in monomer-aggregate equilibrium, directing the Aß assembly away from toxic oligomer formation. The fragments generated by IDE upon cleavage of Aß are aggregation prone but not toxic (Hubin et al. 2016).

Curiously, IDE is regulated by $Aß_{1-40}$ and $Aß_{1-42}$ via a feedback mechanism, which proposes that cells seem to regulate IDE expression to eliminate these toxic peptides (Baranello et al., 2015). Upregulation of IDE expression in the brain of AD transgenic mice has been shown to diminish the amyloid burden and cognitive decline (Kochkina et al., 2015). In agreement, when the IDE gene was selectively deleted in mouse models, these presented key phenotypic characteristics of AD, including chronic elevation of cerebral Aß. An inverse relationship between IDE expression and age has also been reported, what proposes that its loss of activity

may be crucial in the development of AD pathology (Baranello et al., 2015). Indeed, decrease of IDE activity was shown to be linked to AD pathology (Kochkina et al., 2015).

2.2.1.2. Neprilysin

Neprilysin (NEP; aka neutral endopeptidase 24.11 or enkephalinase) is a membrane bound-zinc metallopeptidase synthesized in the Golgi and transported to the cell surface, where it anchors into the extracellular space (Baranello et al., 2015; Li et al., 2015). NEP is included in the group of vasoendopeptidases formed by endothelin-converting enzyme and angiotensin-converting enzyme, the main drug targets for the control of hypertension (Baranello et al., 2015). In fact, NEP cleaves several other substrates due to its wide range of specificity, being the substance P the most efficiently hydrolyzed substrate. Other substrates include enkephalins, atrial natriuretic peptide, tachykinins, bradykinin, adrenomedullin, members of the vasoactive intestinal peptide family, glucagon, thymopentin, and of utmost importance in pathophysiological terms, the Aß peptide (Nalivaeva et al., 2012).

This enzyme is abundant in the kidney but its content in other organs, including the brain, is much lower. In the brain, NEP appears to have mostly neuronal localization especially in the striatonigral pathway, even though it is expressed by activated astrocytes and microglia. NEP was also found in the hippocampus and cortical regions. NEP role in neuronal function is highlighted by its pre- and postsynaptic localization in the nervous system (Nalivaeva et al., 2012). Analysis of the enzyme sequence reveals a type 2 integral-membrane protein structure that starts with a short cytoplasmic domain and a single transmembrane domain that serves as a signal and anchor, followed by a long extracellular domain that set up its catalytic active domain (Baranello et al., 2015).

Along with IDE, NEP is considered to be a major Aß-degrading enzyme with the ability to degrade both monomeric and oligomeric forms of $Aß_{1-40}$ and $Aß_{1-42}$ (Li et al., 2015; Hubin et al., 2016). Several studies have shown that NEP mRNA, protein and activity levels decline with age in the hippocampus and cortex of rodents and humans, and also in the AD brain where senile plaques formation and Aß aggregation was present (Nalivaeva et al., 2012; Baranello et al., 2015; Li et al., 2015). These data suggested that diminished NEP activity during aging might contribute to the development of AD by promoting Aß accumulation. Previous studies have shown NEP inactivation and downregulation during aging and the early stages of AD. Cell culture and *in vivo* experiments revealed an inverse correlation between NEP and Aß levels in AD (Li et al., 2015). Nevertheless, although NEP levels decrease with age and with AD pathology seen in the neuronal cells, it has been demonstrated that NEP is upregulated in reactive astrocytes surrounding amyloid plaques in an AD mouse model (Nalivaeva et al., 2012; Li et al., 2015; Baranello et al., 2015). Age-related decrease of NEP capability to degrade Aß might be due to enzyme oxidation or conformational inactivation, for example, by amyloid peptide (Nalivaeva et al., 2012). Numerous studies demonstrated

that NEP gene therapy in order to increase its levels in AD mice models can decrease Aß plaque formation and preserve brain function (Li et al., 2015).

2.2.1.3. Angiotensin-converting enzyme

Angiotensin-converting enzyme (ACE; aka dipeptidyl carboxypeptidase-1 or DCP-1) is a membrane-bound ectoenzyme, zinc peptidase (Baranello et al., 2015; Larmuth et al., 2016). ACE plays a crucial role in blood pressure and body fluid homeostasis by converting angiotensin I to angiotensin II, and degrading bradykinin (a potent vasodilator). It is mainly secreted in the lung and kidney by cells of the inner layer of blood vessels (Baranello et al., 2015). It is known to cleave a variety of peptides, including Aß peptide and therefore its role in AD. It has been evidenced that ACE is able to inhibit Aß toxicity in cultured cells, by blocking and cleaving the aggregation of Aß (Baranello et al., 2015). Recent studies provided evidence of both endoproteolytic and classical dicarboxypeptidase activities of ACE on Aß peptides (Larmuth et al. 2016).

There are two conflicting hypothesis regarding the correlation between ACE and AD. In order to understand this statement, there are several facts to be considered. Hypertension has been shown to be an important contributor to dementia, including AD, and ACE is a key enzyme in the renin-angiotensin system, which is one of the mechanisms that regulate blood pressure. The amyloid hypothesis proposes that high ACE activity decreases the accumulation of Aß peptide, therefore decreasing the risk of AD. On the contrary, the vascular hypothesis suggests that high ACE-activity increases the risk of AD by increasing blood pressure, consequently leading to cerebral small-vessel disease. Although, Jochemsen and colleagues found a weak and non-significant association between higher ACE activity and more cerebral small-vessel disease, they also suggested that ACE activity would be more indicative and relevant to Aß degradation and brain atrophy (Jochemsen et al., 2015). High levels of ACE protein on the CSF could have a beneficial effect on brain atrophy caused by the Aß burden. Indeed, ACE activity degrades Aß peptide and contributes to less accumulation of Aß into senile plaques in the brain and thereby, reducing the extent of brain atrophy (Jochemsen et al., 2015). In fact, other studies have shown that the level and activity of ACE seems to be increased in AD brains (Baranello et al., 2015).

Several studies suggest that ACE is not a direct physiological regulator of steady-state Aß concentrations in the brain, despite ACE's ability to cleave Aß *in vitro, in vivo* data point out that it does not appear to regulate cerebral amyloidosis (Baranello et al., 2015). Further investigation is needed regarding the role and importance of ACE in the AD pathology.

2.2.1.4. Gelsolin

Gelsolin (GSN) is a highly conserved 89 kD protein whose main function is to sustain the cytoplasmic architecture by regulating the actin filament assembly, and therefore, capping and severing the actin filaments. It is mainly localized in the cell's cytosol and in the plasma, and CSF as secretory protein (Chauhuan et al., 1999; Ray et al., 2000; Hirko et al. 2007;).

The intracellular functions of GSN are regulated by calcium and phosphoinositides (Chauhuan et al., 1999). GSN was also reported to participate in other activities, including modulation of calcium channel and NMDA receptor, apoptosis, and in tumor suppression (Ray et al., 2000). Extracellular GSN functions are not known and studies reported that gelsolin binds to the monomeric form of Aß, and forms an Aß-gelsolin complex. It was proposed as main function of extracellular gelsolin in the plasma and CSF, to sequester and maintain Aß in the soluble form (Chauhuan et al., 1999). Furthermore, Ray and colleagues reported that plasma GSN binds to $Aß_{1-40}$ and $Aß_{1-42}$, and forms a sodium dodecyl sulfate (SDS)-stable complex, which inhibits the fibrillization of soluble $Aß_{1-40}$ and $Aß_{1-42}$ in plasma and CSF. GSN also defibrillizes the performed Aß fibrils in a time-dependent manner, which suggests that GSN plays a vital role in the regulation of Aß fibrillogenesis (Ray et al., 2000). The binding of Aß to GSN is saturable and contains two Aß binding sites. Kinetics of Aß suggest that Aß binding to GSN fits better with two binding sites rather than single binding site. Binding of Aß to GSN is dependent on the concentrations of both GSN and Aß, which is increased with higher concentrations of Aß (Chauhuan et al., 1999). In addition, it was observed that inhibition of GSN gene expression in an AD mouse model was associated with increased apoptotic response in the presence of Aß, demonstrating that interfering with GSN leads to a sensitization to proapoptotic stimuli (Qiao et al., 2004).

Despite GSN having the ability to bind Aß, it was not found in detectable amounts in the amyloid plaques of AD patients (Chauhuan et al., 1999; Ray et al., 2000). Authors suggest that GSN is a major Aß-sequestering protein in the plasma and CSF where it prevents Aß from fibrillization and maintains it in the soluble form (Ray et al., 2000).

2.2.1.5. Transthyretin

Transthyretin (TTR; aka prealbumin) is a homotetrameric protein with a molecular mass of approximately 55 kDa. TTR has an extensive ß-structure, with each monomer being composed of eight ß-strands arranged in an antiparallel configuration. This protein is very stable under physiological conditions both *in vivo* and *in vitro*. The TTR tetramer contains the two thyroid hormones-binding sites and therefore, its main function is to bind and distribute thyroid hormones (THs) (Alshehri et al., 2015). TTR transports thyroxine (T4) and retinol, by its association with retinol binding protein (RBP), apolipoprotein A-I, neuropeptide Y, and a panoply of exogenous disrupting chemicals and drugs, in CSF and plasma (Alshehri et al.,

2015; Ciccone et al., 2016). TTR is mainly synthesized in the liver and in the choroid plexus (Ciccone et al., 2016; Alemi et al., 2016). Regarding the liver, TTR is secreted into the bloodstream and distributes the thyroid hormones around the body, whereas TTR synthesized in the choroid plexus is involved in the movement of thyroxine from the blood into the cerebrospinal fluid and distribution of THs in the brain (Alshehri et al., 2015).

TTR was described as the major Aß binding protein in the CSF by Schwarzmen and colleagues. These authors proposed that TTR was able to inhibit aggregation and toxicity of Aß, suggesting that when TTR fails to sequester Aß, amyloid formation take place (Schwarzmen et al., 1996). In fact, new roles for TTR have been suggested such as protection against neurodegeneration, involvement in behavior, memory and learning, and also promotion of neurodegeneration. It has been recently discovered that TTR may play a wide role in neurobiological function due to the high number of chemicals that can bind to TTR, therefore, interfering with its functions in the brain. TTR is associated with a growing list of neurological diseases including AD, depression, anxiety, schizophrenia, familial amyloid polyneuropathy and familial cardiomyopathy (Alshehri et al., 2015; Ciccone et al., 2016).

There are some theories concerning the TTR mechanism associated to the prevention of AD: (i) TTR has a direct role in AD by sequestering Aß and thus preventing amyloid formation; (ii) in late onset AD patients, diminished TTR in the CSF results in an increase in the Aß fiber formation; (iii) it was suggested, as an indirect role for TTR, that it prevents Aß formation in the amyloidogenic pathway by inhibiting the cleavage of the CTF99 by γ-secretase (CTF99 is responsible for the release of the Aß peptide); (iv) TTR facilitates the non-amyloidogenic pathway by increasing α-secretase to cleave APP, which results in the production of sAPPα (Alshehri et al., 2015). TTR levels have been shown to be decreased in both CSF and plasma in aging and in AD patients, which supports the idea of neuroprotection by TTR (Alemi et al., 2016). Curiously, authors demonstrated that TTR expression is increased in some neurons of the AD brain. The multiplicity of molecular mechanisms involving TTR interactions with Aß peptides and their precursor seems to clarify why TTR expression is increased in some neurons of the AD brain (Li et al., 2016).

2.2.1.6. Metallothioneins

Metallothioneins (MTs) are the major endogenous zinc- and copper-binding proteins present in the brain and play a crucial role in maintaining metal homeostasis (Chung et al., 2010). MTs are high cysteine and metal content cadmium-binding proteins. MTs are subdivided into numerous families based on primary sequences. Mammals possess several isoforms, including MT-1, MT-2, MT-3, and MT-4. The first three isoforms are known to be synthesized in the central nervous system (CNS), composed of a single polypeptide chain, of which some of them are cysteine residues (Manso et al., 2011). The MT-2A isoform is the most expressed isoform of MTs and is described as a neuroprotective protein essential for brain repair and represents

the MTs (Chung et al., 2010). The *Mt-2A* gene is widely expressed and can be found throughout the brain and spinal cord, and is mainly expressed by the astrocytes, with lower levels of expression in ependymal cells, epithelial cells of choroid plexus, meningeal cells of the pia mater, and endothelial cells of blood vessels. MT-2 has been reported to be synthesized in neurons but in very low levels compared to astrocytes (Manso et al., 2011).

MT-2A is a neuroprotective protein, via intracellular functions that include metal detoxification and quenching of oxidative free radicals (Chung et al., 2010). The MT-2A isoform amino acids typically bind seven divalent metal ions [Zn(II), Cd(II)] and up to 12 monovalent copper ions through thiolate bounds. These metals are separated into two metal-thiolate clusters holding three and four divalent metal ions or six monovalent metal ions each (Manso et al., 2011). MT-2A isoform is upregulated in neuroinflammatory environments, as can be caused by the neuropathology of AD. MT-2 expression levels are highly regulated by cytokine interleukine-6 (IL-6), which is a neuroinflammatory factor. This MT isoform has been suggested to have a role has antioxidant, anti-inflammatory, and antiapoptotic, in addition to its zinc and copper binding capabilities, underlying MT-2A neuroprotective activities (Manso et al., 2011).

MT-2A expression is significantly upregulated in regions where Aß plaque burden is present in the pre-clinical and clinical AD brain, as well as in the brains of an AD mouse model (Chung et al., 2010). The upregulation of this protein in the surrounding area of the amyloid plaques will benefit the nearby cells, considering the antioxidant, anti-inflammatory and antiapoptotic assets of MT-2A. This MT is also a metal binding protein, a very important property in this case since Aß plaques are enriched with zinc, copper, and iron, which are metals probably involved in the aggregation of Aß (Manso et al., 2011). Studies demonstrated that Zn_7-MT-2A, can prevent the Cu-mediated aggregation of Aß 1-42 although Zn_7-MT-2A is incapable of de-aggregate either Cu-$Aß_{1-42}$ or Cu-$Aß_{1-40}$. Based on different data, the same authors predicted that the zinc bound is required for the ability of MT-2A to block copper mediated $Aß_{1-40}$ and $Aß_{1-42}$ aggregation, due to the existence of a metal exchange of copper and zinc between Zn_7-MT-2A and Cu(II)Aß. This observation might be explained by the MTs ability of higher binding affinity metals (copper) to shift lower affinity metals (zinc). The same authors also observed that Zn_7-MT-2A is able to protect against Cu(II)-Aß induced neuronal degeneration, again due to the metal exchange of copper and zinc (Chung et al., 2010; Manso et al., 2011).

3. Circadian rhythm

Circadian rhythms are defined as oscillations with a periodicity of approximately 24h and constitute a fundamental component of mammalian physiology. These internal circadian clock systems have the function of coordinating to external synchronizing cues (Zeitgebers), such as the light-dark cycle (Thome et al., 2011; Musiek et al., 2015). The circadian system commands the 24h rhythmicity in sleep-wake cycle, body temperature, feeding, rest-activity behavior, hormonal levels, among other biological processes of the organism (Videnovic et al., 2014).

3.1. Human circadian rhythm model, components and location

The suprachiasmatic nucleus (SCN) characterizes the core of the circadian system, being the main component and represents the master clock of the circadian system (Cassone et al., 1988; Videnovic et al., 2014). The SCN can be divided in two parts: a core and shell subnuclei. The subnucleus has distinct neurochemical properties, containing γ-aminobutiric acid (GABA) which is the main neurotransmitter in almost all neurons of the SCN. Neurons present in the SCN core secrete vasoactive intestinal polypeptide (VIP), whereas neurons in the shell secrete arginine vasopressin (Dardente et al., 2007; Golombek et al., 2010; Videnovic et al., 2014; Musiek et al., 2015). The arginine vasopressin works in a complementary manner to impart stability and flexibility to the circadian timing system (Saper, 2013; Wang et al., 2015). The role of the VIP neurons of the SCN core is to obtain direct light input from the retina and to deliver intranuclear projections to the rest of the SCN itself (Wang et al., 2015).

The circadian timekeeping is arranged by complex molecular loops and is composed by three distinct components: a pacemaker (SCN), afferent pathways (for light and other stimuli that synchronize the pacemaker to external cues) and efferent output rhythms regulated by the SCN (Videnovic et al., 2014). The SCN will signal via multiple mechanisms, including the autonomic nervous system and hormone release, to synchronize cell-autonomous peripheral clocks in the body (Weaver, 1998; Musiek et al., 2015). The SCN must be able to afford a steady, robust circadian output while remaining adaptable to differences between endogenous and exogenous cycles that arise from seasonal changes in the time of sunrise and endogenous circadian periods not exactly equal to 24h in length (Wang et al., 2015).

One of the most apparent example of a circadian process is the sleep-wake cycle, which occurs with a consistent 24h rhythm and can be shifted according to environmental cues (Musiek et al., 2015). Circadian rhythmicity, can also be observed in body temperature, and

secretion of numerous hormones, red blood cells production and other physiological parameters (Volicer et al., 2012). The rhythmic clock gene expression has been described, in humans, in peripheral tissues such as skin, oral mucosa, colonocytes, bone marrow, heart, and white blood cells but there's very few information on human brain oscillators (Cermakian et al., 2011). It is thought that the one of the main reasons for the global disruption of the body´s circadian activity is directly linked with decreased electrical, hormonal and gene-expression activity of SCN cells which is associated with aging (Costa et al., 2013). The circadian clock controls many pathways involved in neurodegeneration, such as autophagy, metabolism, reactive oxygen species (ROS) homeostasis and oxidative stress response and DNA damage repair (Costa et al., 2013).

The SCN is able to preserve these 24h rhythms in physiological functions through a complex molecular based mechanism (Videnovic et al., 2014).

3.2. Circadian rhythm molecular mechanisms

The regulation of the circadian rhythms depends on a set of clock genes, including circadian locomoter output cycles kaput (CLOCK), brain and muscle Arnt-like protein-1 (BMAL1) or aryl hydrocarbon receptor nuclear translocator-like (ARNTL), three PERIOD genes (PER1, PER2, and PER3) and two plant CRYPTOCHROME gene homologues (CRY1 and CRY2). These genes have the very important task of controlling a considerable percentage of the genome: approximately 10% of all expressed genes estimated to be regulated by the clock genes. These genes can be considered ubiquitous, as almost all peripheral tissues, including brain regions outside the SCN, contain autonomous circadian clocks. These clocks are most likely synchronized by the SCN but they also can be influenced by their own distinct circadian synchronizers (Videnovic et al., 2014).

The maintenance of the circadian rhythms in the SCN in most cells is made by a cellular clock transcriptional machinery involving the bHLH/PAS transcription factors ARNTL and CLOCK. These two heterodimerize and drive transcription of several genes which includes their own negative feedback repressors PER and CRY genes; these last ones repress BMAL1/CLOCK-mediated transcription (Mohawk et al., 2012; Musiek et al., 2015). This feedback loop functions as a regulator and can be divided into positive and negative limbs. The positive limb comprises the CLOCK and ARNTL, two PAS helix-loop-helix transcription factors; they form heterodimers and bind to E-box enhancer element, thus, are able to regulate the transcription of both PER and CRY genes. The negative limb comprises PER and CRY proteins, and its main function is to attenuate activation of their own genes by CLOCK/BMAL1, consequently producing the negative feedback (Figure 2; Abe et al., 2002; Kunieda et al., 2006; Marpegan et al., 2011; Musiek et al., 2015). More specifically, the intracellular level of CLOCK remains the same throughout the 24 h period. There is a peak of ARNTL expression at the beginning of the day that promote the formation of ARNTL–CLOCK heterodimers, which

will activate transcription of PER and CRY. As PER accumulates in the cytoplasm, it becomes phosphorylated and degraded by ubiquitylation. CRY accumulates in the cytoplasm late in the subjective day, and translocates to the nucleus to inhibit ARNTL–CLOCK-mediated transcription. At night, the PER–CRY complex is degraded, and the cycle starts again. This feedback loop ensures a high level of ARNTL and low levels of PER and CRY at the beginning of a new circadian day (Figure 2) (Videnovic et al., 2014).

An important feature of CLOCK genes is their close interrelation with external, environmental factors because very few other gene families demonstrate such strong environment affiliation and interdependency. Consequently, they are highly subjective to exogenous factors (such as stress) and endogenous vulnerability factors, such as inherited genetic variants, eventually leading to the clinical phenomenology of AD (Thome et al., 2011).

One aspect to keep in mind is that it is extremely difficult to monitor CLOCK genes, either one monitors the genes themselves or their RNA or protein products. Regarding the gene level, it is important to know exactly when the material was collected during the day. As it is known the genes are under the influence of circadian rhythms, a sample collected during the day will be different from the one collected during the night and *vice-versa*. Finding a matched control is also difficult. It is also important to eliminate false positives and false negatives during background subtraction and data manipulation, which can be difficult to address (Thome et al. 2011).

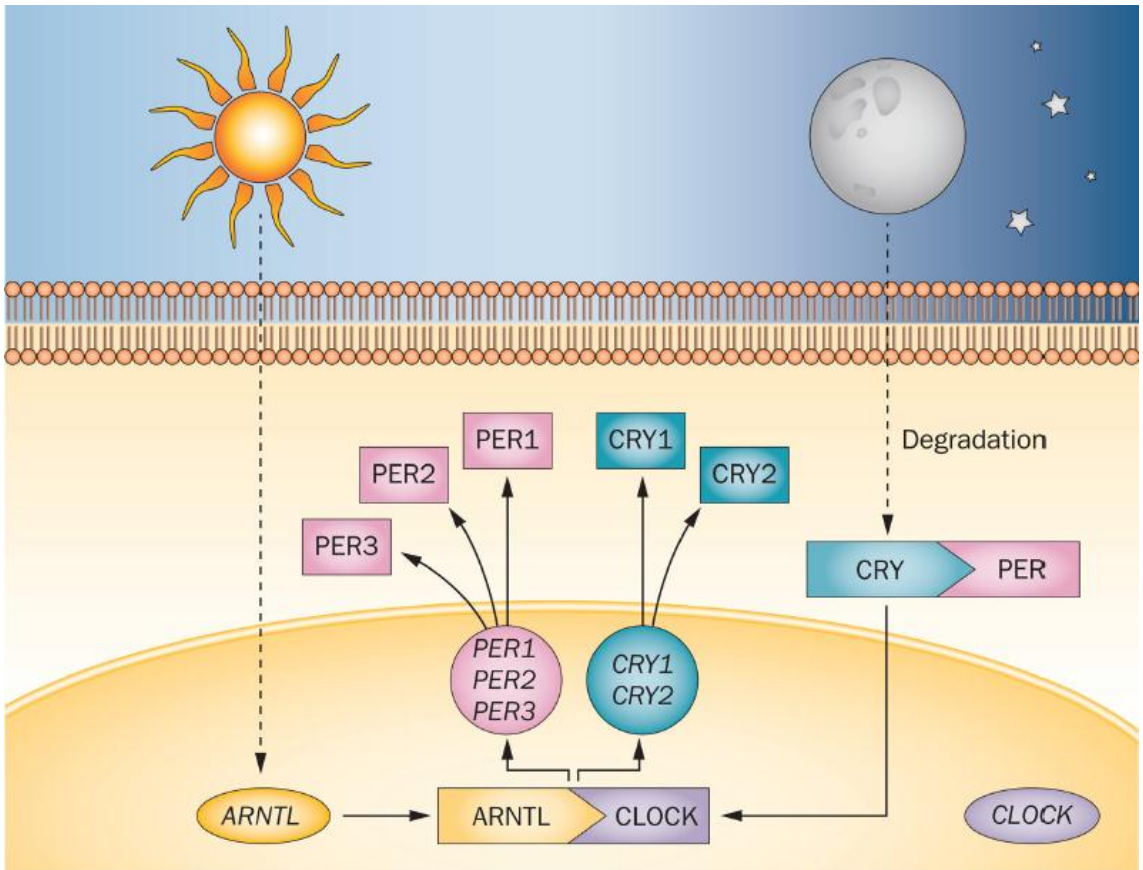

Figure 2 – Molecular mechanism of the circadian system. The proteins encoded by the core set of clock genes—PER, CLOCK, BMAL1/ARNTL and CRY—cooperate to create a self-sustaining negative transcription–translation feedback loop (adapted from Videnovic et al., 2014).

3.3. Circadian rhythmicity, sleep disturbances and AD

One of the most common features in AD are sleep and circadian rhythm disturbances, and it has been reported that up to 45% of patients may have sleep problems. Excessive awakenings (23%), excessive daytime sleepiness (10%), early morning awakening (11%), and napping for more than 1 hour during the day (14%) makes the most of the major disturbances. These features can be present early in the progression of the disease, despite the fact that they tend to be correlated with the severity of the cognitive decline (Urrestarazu and Iriarte, 2016). Circadian clock malfunction has a major influence in sleep and it is thought to make changes that influence memory formation and cognitive functions, which are sleep-dependent processes (Costa et al., 2013; Musiek et al., 2015). Indeed, sleep has a very important role in restoring the functions of the brain and it is involved with memory retention (Born and Wilhelm 2012; Lucey and Bateman, 2014). It has been observed that in extreme cases, a complete day/night sleep pattern reversal can occur (Urrestarazu and Iriarte 2016). Circadian clock disruptions also leads to reduced amplitudes and phase delay of circadian variation in core body temperature and activity. As a result of these circadian alterations, patients show increases in cognitive decay/dementia, number of daytime naps, wandering, nocturnal insomnia, misperception and disorientation, and decreases in motor control and metabolism (Costa et al., 2013; Videnovic et al., 2014). The changes in body temperature rhythms have been evidenced to differ between genders in older subjects, as alterations have their amplitude reduced in older males, but not in older females (Costa et al., 2013).

Studies monitoring the sleep-wake cycle in cognitively normal individuals aged between 45-75 years revealed decreased sleep efficiency and increased nap frequency in individuals with amyloid deposition in comparison with those of the same age deprived of amyloid deposition, determined by CSF Aß42 levels (Ju et al., 2013; Lucey and Bateman, 2014). It was shown that individuals cognitively normal shared a statistically significant difference in sleep parameters when separated by amyloid deposition status which supports the hypothesis that sleep disturbances are associated with AD pathology and precede the onset of cognitive impairment (Lucey and Bateman, 2014). In addition, in animal models the levels of soluble Aß are higher in the ISF of APP transgenic mice during wakefulness and lower during sleep. These mice have a normal sleep cycle when younger and before amyloid deposition. Then, when the Aß plaque formation in APP transgenic mice begins, a loss of the Aß diurnal pattern is observed and also an obvious disrupted sleep-wake cycle with increased wakefulness and sleep during the light phase when the mice should be sleeping. These findings regarding sleep alterations in transgenic mice indicate that the irregularities in sleep are due to Aß aggregation in the brain (Roh et al., 2012; Lucey and Bateman, 2014). Also, sleep deprivation of mice for 21 days

increased ISF Aß concentrations and accelerated Aß deposition into plaques. (Kang et al., 2009; Lucey and Bateman, 2014). In addition, other authors evidenced that the levels of soluble Aß in the extracellular ISF of the hippocampus in mice are dynamically and positively related with minutes awake per hour and negatively related with time asleep (Kang et al., 2009; Roh et al., 2014; Ju and Holtzman, 2013; Ooms et al., 2014; Roh et al., 2014). Two different authors demonstrated a 12 and a 15% increase in the sleep time during the dark phase that was related with more than 50% reduction in the progression of Aß pathology in the brain (Yan et al., 2009; Roh et al., 2014). Observations with transgenic mice, when they were kept in standard 12h:12h light:dark conditions, the levels of Aß were highest during the dark phase (period of mice activity) and lowest during the light phase (period of mice sleep; Musiek et al., 2015). These studies are in agreement with others where it has been reported that neurodegenerative disorders, such as DA, disrupt the circadian clock and these internal time alterations are very likely to be one of the primordial signs of the disease (Costa et al., 2013).

Regarding the molecular basis of the circadian rhythm, the deletion of the master clock gene *BMAL1* annuls all circadian function which leads to a total loss of day-night rhythmicity of sleep (Bunger et al., 2000; Laposky et al., 2005; Musiek et al., 2015). Sleep deprivation can modify the expression of clock genes and also the DNA binding patterns of BMAL1/CLOCK heterodimers, consequently changing clock function (Mongrain et al., 2011). Recent studies suggest the mechanism of Aß induced circadian rhythm disruption is by enhancing the degradation of BMAL1, leading to disruption of PER2 expression at both protein and mRNA levels (Song et al., 2015). Aß destabilizes BMAL1 and CBP proteins by sumoylation, a post-translational modification (Cardone et al., 2005; Song et al., 2015). Sumoylation is present during oxidative-stress and Aß peptide is able to activate the enzymes that lead to sumoylation of BMAL1 and, therefore, to its degradation and thereby the circadian rhythmicity (Song et al., 2015). Numerous studies in humans have suggested that circadian dysfunction in AD lies on the disruption and degeneration of the SCN (Harper et al., 2008; Farajnia et al., 2012; Musiek et al., 2015).

Sleep can limit Aß production as well as regulate the clearance of Aß from the brain. Sleep actually induces significant increases in the volume of extracellular fluid in the brain and promotes the convective bulk flow of metabolites and proteins out of the brain, a process controlled by glia (Xie et al., 2013; Musiek et al., 2015).

4. Choroid plexus

4.1. Choroid plexus location and structure

The choroid plexus (CP) is a highly vascularized tissue located within each ventricle of the brain, the lateral, third and fourth ventricles. Structurally, the CP is made of the telencephalic CP in each lateral ventricle, the diencephelic CP of the third ventricle and the hindbrain CP (Figure 3A; Liddelow, 2005; Lun et al., 2015).

The endothelium capillaries of the CP are fenestrated, and are connected by thin membranous diaphragms permeable to small molecules and water, which enables the rapid delivery of water from the blood to epithelial cells for CSF production. The solutes seem to cross from the blood into the stromal space by diffusion across endothelial fenestrae or by vesicular transport (Lun et al., 2015). The structure of CP mirrors consists on a monolayer of cuboidal cells that surrounds a stromal core of capillaries and connective tissue. The blood-CSF barrier (BCSFB) is formed by the adjacent CP epithelial cells joined together by tight junctions. This barrier prevents paracellular free passage of molecules from the systemic circulation into the CSF. The tight junctions, along with adherens junctions, guarantee the apico-basal polarity of membrane proteins, such as transporters, which play a key role for normal epithelial cell function (Damkier et al., 2013; Lun et al., 2015). The BBB, one of the main brain defense barriers, entails the tight junctions-containing endothelial cells of the brain capillaries, and the BCSFB is formed by the epithelial cell monolayer of the CP, located in the brain ventricles. The BBB entails the tight junctions-containing endothelial cells of the brain capillaries, and the BCSFB is formed by the epithelial cell monolayer of the CP, located in the brain ventricles (Demeestere et al., 2015). This epithelial cell monolayer locates in a basal lamina surrounding and enclosing a central stroma with dendritic cells, fibroblasts and macrophages (Marques et al., 2015). Attached to the apical side of CP epithelial cells, are present the epiplexus cells. These cells possess macrophage activity and examine the CSF filled brain ventricles and there are also present, supraependymal cells. These cells, in conjunct, play a key role in defensing the brain from infections, after bacteria transverse the CP (Figure 3B; Marques et al., 2015).

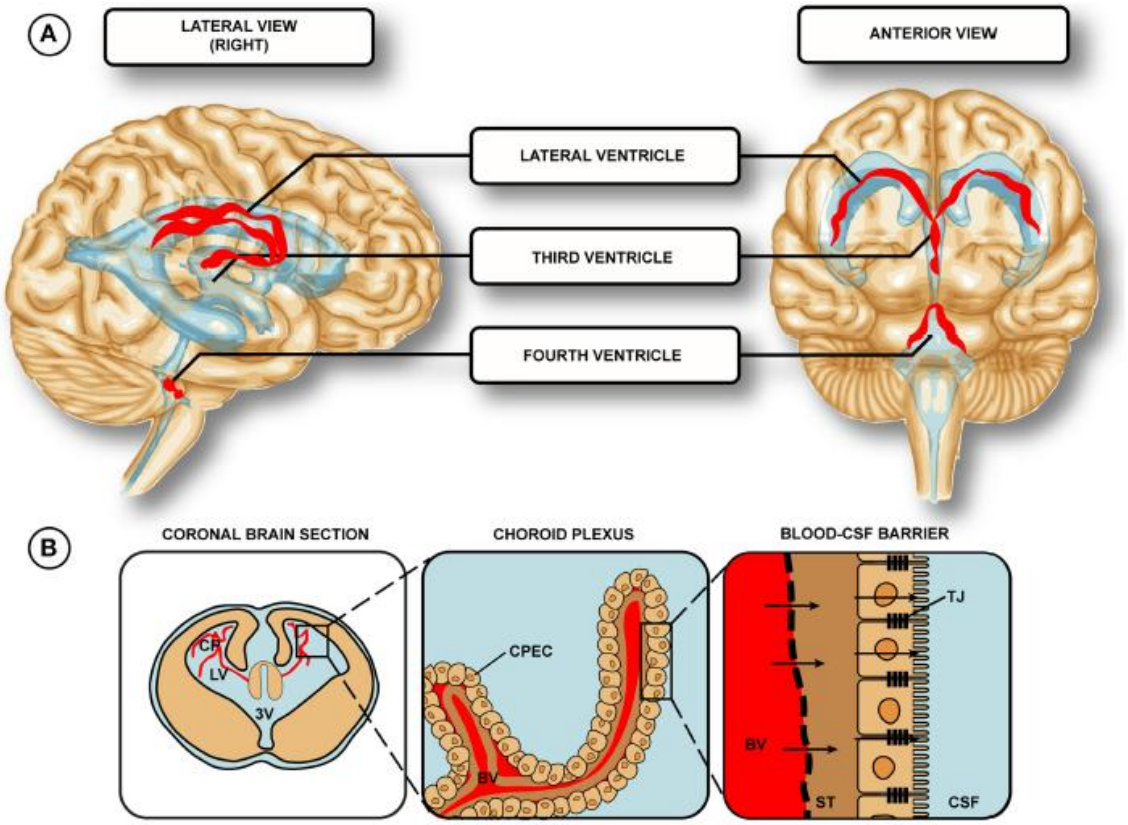

Figure 3 – Location of the CPs in the human brain. A) The CPs are present in the two lateral, third and fourth ventricles (red bands). B) Every plexuses contain fenestrated vessels, with a single layer of closely opposite CP epithelial cells, joined by tight junctions which forms the blood-cerebrospinal fluid barrier (BCSFB; adapted from Liddelow, 2015). Abbreviations: BV, blood vessel; CPEC, choroid plexus epithelial cell; CSF, cerebrospinal fluid; LV, lateral ventricle; ST, stroma/basement membrane; TJ, tight junction; 3V, third ventricle.

4.2. Choroid plexus function

The CP perform a multitude of functions such as synthesis, secretion, active transport and selective reabsorption of deleterious substances (Lun et al., 2015). CP main function is to produce CSF in the vertebrate brain and to maintain the extracellular environment of the brain by monitoring the chemical exchange between the CSF and the brain tissue (Krzyzanowska et al., 2012; Lun et al., 2015). This monitoring involves the surveying of both chemical and immunological status of the extracellular fluid and the removal of toxic substances as well as important roles in the regenerative processes following traumatic events. The CP is also capable of producing various peptides which can have beneficial and neuroprotective properties, as well as monitor and maintain the biochemical and cellular homeostasis of the central nervous system (CNS) (Krzyzanowska et al., 2012).

Approximately two thirds of the CSF is produced and secreted by CP, the remaining part is produced by other brain regions, including the ependymal cells of the ventricular surface and those cells lining the subarachnoid space (Liddelow, 2005). The production of CSF by the CP

occurs by passive filtration of fluid across the extremely permeable capillary endothelium and regulated secretion across the CP endothelium (Demeestere et al., 2015). The CP-CSF system is the upmost system for the development and maintenance of the CNS. Several studies had showed the importance of a proper CP function to the formation and integrity of the CNS. Lack of CSF causes an impaired brain growth, due to the right CSF pressure during normal brain development. On the other hand, an excess of CSF, caused by overproduction, obstructed flow or even limited CSF reabsorption, can cause hydrocephalus (excess accumulation of CSF within the brain ventricles) (Lun et al., 2015).

4.3. Choroid plexus role in Alzheimer's disease

The CP is highly sensible to the many external factors and goes through structural and physiological changes during aging and disease states. Harmful changes in the CP's anatomy, function and also CSF turnover have been found in several neurological diseases, including AD (Alvira-Botero and Carro, 2010). The CP plays a key role in the most basic features of neural function, such as Aß clearance by expressing several Aß-scavengers (as mentioned previously in section 2.2) (Carro et al., 2002; Zlokovic, 2004; Vargas et al., 2010). It was shown that $Aß_{1-42}$, the most neurotoxic form of the Aß peptides, modifies BBB integrity and causes a significant increase in NO production which is implicated in the AD pathogenesis (Zhang et al., 2002; Keil et al., 2004; Teng and Tang, 2005; Vargas et al., 2010). Oxidative stress, and more specifically, oxidative protein damage is present in the early onset of the disease. It may affect protein interactions, protein folding and protein kinase activity, abnormal functions of endothelial and vascular smooth muscle cells, and impaired HDL cholesterol metabolism, therefore having important implications in the deterioration of the CP's functions (Perez-Garcia et al., 2009; Krzyzanowska et al., 2012).

In AD the CP develops irregularities similar to those related with aging, however very enhanced. Indeed, CP ability to secrete Aß-carrier and scavenger proteins and to express important receptors that scavenge Aß peptides is decreased with age and is compromised in several models of AD (Zlokovic et al., 1996; Krzyzanowska et al., 2015).

Accumulation of amyloid-like inclusions, also known as Biondi ring tangles in CP epithelial cells, might affect vital function of the CP in AD cases (Wen et al., 1999; Vargas et al., 2010). Those alterations such as epithelial atrophy of the CP (Serot et al., 2000), which is significantly accentuated in AD, may alter the choroid plexus main functions, including synthesis, secretion, and transport of proteins to other molecules. This is considered by many authors not to be enough to cause amyloid deposits in the majority of AD cases but plays a key role in the initiation and development of AD pathology. Additionally, authors hypothesize that disturbed CP functions may precede several AD hallmarks, such as amyloid brain accumulation. The altered CP function could be one of the primary pathogenic events in late-

onset AD (Krzyzanowska et al., 2012). In the LOAD stage there are numerous CP significant modifications such as epithelial atrophy, fibrosis, and thickened basement membranes which proposes a disruption on CP functions (Bolos et al., 2014).

Aß peptide also accumulates in the CP of autopsied AD patients, and suggested a direct relationship between Aß deposits at CP epithelium and the development of a functional and structural disruption of the organ (Dietrich et al., 2008; Krzyzanowska et al., 2012). Vargas and colleagues also revealed the presence of Aß accumulation in CP of APP/PS1 transgenic mice and AD patients, and demonstrated its association with transcytosis impairment, increased nitric oxide (NO) production and cell death mediated by mitochondrial dysfunction. They showed that Aß deposits were responsible for mitochondrial dysfunction in CP and also a direct effect of Aß accumulation on cell death induction in CP (Vargas et al., 2010). Aß can be found in CP epithelial cells from non-demented subjects, although the proportion of epithelial cells containing Aß accumulation increases considerably in CP from AD patients (Krzyzanowska et al., 2012). The decreased activity of the enzymes involved in oxidative phosphorylation and mitochondrial activity might help to disrupt the protein synthesis in the CP. The impairment of the functional activity of the CP is associated with the decrease in protein secretion and renewal of the CSF, which can also be involved in the onset and progression of AD (Liu et al., 2013; Krzyzanowska et al., 2015).

Interestingly, recent studies have shown that Aß has the ability to stimulate neural progenitor cells within the CP through prompting endogenous growth factor actions. Aß peptide can induce neurogenesis, however many of these newly born neurons die shortly after differentiation which suggests that the neurons do mature but undergo cell death. Nevertheless, further results suggest that amyloidogenic environment tends to down-regulate neurogenesis (Bolos et al., 2013).

Due to the variety of the CP's functions, even a slight modification in the CP can promote extensive effects. Modifications in the CP's anatomy and physiology are linked with ageing and many others central nervous system diseases, comprising AD and are parallel with abnormal brain activity (Serot et al., 2003; Vargas et al., 2010).

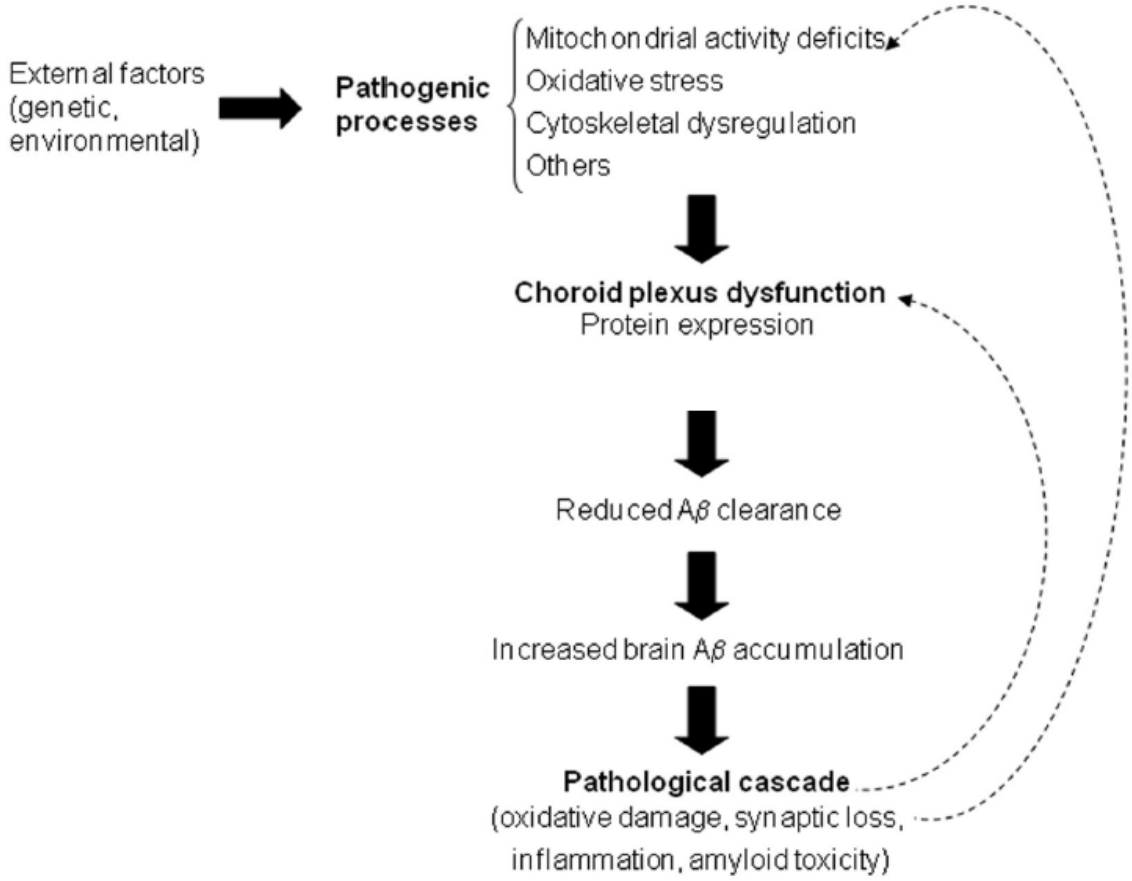

Figure 4 – **Proposed sequence of pathological events in Alzheimer's disease** – Several pathogenic processes contribute to the dysfunction of the choroid plexus which results in a disrupted Aβ processing. These processes plus the accumulation of Aβ contributes to the development of the pathogenic progression (Adapted from Krzyzanowska et al., 2015).

II. AIM

The work hypothesis in this study was that the circadian rhythm and AD progression regulate the expression of Aß-scavengers in CP of AD patients. For that purpose, the global aim was to analyze the expression of Aß-scavengers in the CP of AD patients. This current work has the following specific objectives:

1. Design primers specific for IDE, NEP, ACE, GLS, TTR and MT2A, CLOCK, BMAL1, PER2, PER3 and CRY2 genes;
2. Optimize RT-qPCR reactions for the Aß-scavengers and circadian rhythm genes;
3. Analyze relative mRNA levels of expression of TTR, GLS and NEP genes in CP of AD patients at different Braak stages by comparison to age-matched controls.

III. MATERIALS AND METHODS

1. Samples

Choroid plexus tissue was obtained from Department of Patahology and Neuropathology (Xerencia de Xestión Integrada de Vigo-SERGAS, Spain) and Neuropathology Brain Bank (HUB-ICO-IDIBELL Biobank), and Banco de Tejidos. All samples were obtained following the ethical guidelines both of Spanish legislation on this matter and of the local ethics committee. The post-mortem interval between death and tissue processing was between 3 and 14 hours. Neuropathological diagnosis of AD was based on the Braak classification, mentioned in the introduction. Samples are represented in table 1, above.

Table 1 – Patients samples characteristics, including age and Alzheimer's disease Braak stage.

Number of sample	AD Braak Stage	Age	Gender
1	Control	44	
2	Control	40	
3	Control	52	
4	Control	52	Male
5	Control	80	
6	Control	63	
7	Control	28	
8	AD I	64	
9	AD I	68	
10	AD I	64	
11	AD I	58	
12	AD I	76	
13	AD I	63	
14	AD I	63	
15	AD II	55	Male
16	AD II	57	
17	AD II	60	
18	AD II	83	
19	AD II	74	
20	AD II	86	
21	AD III	73	
22	AD III	81	
23	AD III	77	
24	AD III	82	
25	AD V	82	Male
26	AD IV	79	
27	AD III	76	
28	AD V	75	

2. RNA extraction

2.2. Total RNA extraction

Extraction of total RNA (tRNA) from the human CP samples was carried out with maximum care and on ice due to easy enzymatic degradation of RNA and the sensitive response of RNA to temperature.

Before starting the procedure, all instruments were properly cleaned with a RNA surface decontaminant to reduce the level of contamination (RNase AWAY®, Molecular BioProducts). The first step of the procedure was to slowly thaw the CPs samples on ice to prevent RNA degradation, followed by trituration with a bistoury. After transferring the sample to the glass tube it was homogenized in 1 mL TRIzol® Reagent (Thermo Fisher Scientific) using a glass pestle against the tube wall creating maximum traction to allow fully trituration and separation of the cellular components. After homogenization the sample was transferred to an eppendorf tube using a plastic disposable pipette, properly sterilized, and followed by incubation for 5 minutes at room temperature (RT) for complete dissociation of nucleoprotein complexes. Then, 200 µL of chloroform (200 µL chloroform per 1 mL TRIzol) were added followed by 15 seconds of vigorous manual agitation. Afterwards, samples were again incubated for 2-3 minutes at RT followed by centrifugation at 4^0C for 15 minutes at 12 000 G (Legend Micro 21 R Centrifuge, Thermo Scientific). This centrifugation enabled separation of the solution in three different phases. The transparent aqueous phase, the one containing RNA, was carefully collected and transferred to a new eppendorf tube. This step requires accuracy to only collect the transparent phase to prevent further contamination of the sample with genomic DNA. Then, 500 µL of isopropanol 100% (500 µL isopropanol per 1mL TRIzol) were added with proper homogenization of the solution, followed by incubation for 10 minutes at RT. Next, samples were centrifuged at 4^0C for 10 minutes at 12 000 G and the supernatant discarded. This step also requires a careful handling due to the presence of RNA in white form, which is the pellet, to not be discarded along with the isopropanol. The RNA pellet was washed with 1 mL of ethanol 75% in sterile water (from B. Braun Medical SA), followed by vortex homogenization. Samples were further centrifuged for 5 minutes at 4^0C for 7 500 G followed by rejection of the supernatant, again, carefully to not discard the RNA. The next step is to let the sample dry the remaining ethanol in the sample for 10-30 minutes at RT with the tube inverted. This step will prevent further ethanol contamination of the sample. Afterwards, the RNA sample was rehydrated in 20 µL of RNAse Free Water (from Qiagen GmbH) and properly homogenized. Finally, the sample was incubated for 60^0C for 10-15 minutes with agitation in the thermal cycler (Thermomixer Compact, Eppendorf). The sample was stored at -80^0C for later use.

tRNA was quantified by using a nanospectrophotometer (Nanodrop Technologies, USA). This apparatus is capable of giving directly the concentration (ng/µL) of the tRNA solution by pipetting 1 µL for further reading, and it also gives the ratios of absorbance at 260/280 nm and 260/230 nm. To confirm the quality of the tRNA, it is considered pure when the 260/280 ratio is between 1,8 and 2,0. If the ratio is under 1,8 the tRNA is contaminated with proteins, which can lower further reaction efficiency. A 260/280 ration close to 2,0 is generally accepted as pure for RNA. The 260/230 ratio evaluates the carryover of components containing phenol rings, which are inhibitory to enzymatic reactions. The values for pure RNA for this ratio are often higher than the 260/280 values. Expected 260/230 values are commonly in the range of 2,0-2,2, if the ratio is lower than expected, the RNA may be contaminated with phenol or even TRIzol.

The integrity of tRNA was also tested by electrophoresis on 1% agarose gel. The tRNA quality was confirmed by the presence of two bands in the gel, 18S and 28S. The 28S band is twice as bright as the 18S band, and when the tRNA is degraded, this proportion might be affected.

3. Reverse-transcription – cDNA synthesis

Complementary DNA (cDNA) synthesis was performed by reverse transcription reaction of mRNA. It was used an iScript™ cDNA Synthesis Kit (Bio-Rad) for this purpose, according to the fabricant recommendations. In brief, for a 40 µL of total reaction volume, it was used 8 µL of 5x iScript reaction mix, 2 µL of 1x iScript Reverse Transcriptase and sterile water (from B. Braun Medical SA) until performing the total volume of the initial mixture. Lastly, it was then added 1 µg of tRNA for each sample, followed by proper mix of the solution. All steps were performed on ice. The samples were incubated on a thermal cycler (PTC-200 Peltier Thermal Cycler, MJ Research) at 25^0C for 5 minutes, followed by 42^0C for 30 minutes and, lastly, at 85^0C for 5 minutes. The samples were further stored at -20^0C for later use.

4. Polymerase-chain reaction (PCR)

4.1. Primer design

The primers for each gene in the current study were all designed from scratch. For this procedure it was used a specific program, PrimerBlast

(http://www.ncbi.nlm.nih.gov/tools/primer-blast/), using several minimum requirements by following detailed steps for the obtainment of the best primers possible, regarding its thermodynamics and specificity.

Step 1 – Search for accession number (NM) for each gene: In the PubMed website (http://www.ncbi.nlm.nih.gov/pubmed), click on the "Nucleotide" database. Insert the gene name and the type of organism in which the primers will be specific by clicking "Homo sapiens" in the option "Results by taxon".

Step 2 – Using PrimerBlast Program: once having the NM of the gene, it is necessary to use the PrimerBlast program. After putting the NM of the gene in the proper box, it is possible to choose several different factors in order to obtain efficient primers.

●Primer parameters:

PCR product size: should be between 70 bp and 200 bp due to the use of SYBR Green dye in real-time qPCR.

Primer melting temperatures (T_m): the optimum temperature is between 59 - 61^{0}C. The difference between forward and reverse primers should be 1^{0}C or less.

Primer length: it is accepted that the optimal length of PCR primers is between 18-22 bp.

GC Content: The GC content (the number of G's and C's in the primer as a percentage of the total bases) of primers should be between 45-60%. High GC content may not denature well during cycling and also susceptible to non-specific interactions. It is important that the primers contain no internal secondary structure, and have a balanced distribution of G/C and A/T rich domains.

●Exon/Intron Selection:

These primers are designed to be able to bind separate exons, they have intron/exon junctions.

●Primer Pair Specificity Checking Parameters:

Database: choose the "Refseq RNA (refseq_mrna)" option.

Organism: here we choose for what type of organism the primers will be specific, in this case it will be "Homo sapiens".

Primer Pair Specificity Checking Parameters: click on "Allow primer to amplify mRNA splice variants (requires refseq mRNA sequence as PCR template input)".

Now it is necessary to click on the "Advance parameters" option.

●Primer Parameters

Max Self Complementarity: This option should be “Any = 4” and “3’ = 1”.

Max Pair Complementarity: This option should be “Any = 4” and “3’ = 1”.

It is necessary to take into account that the primers should not be complementary to each other at their 3’ ends and that are not self-complementary. Primer-dimers will form if the primers have one or more complementary bases so that base pairing between the 3’ ends of the two primers can occur. It is only allowed a maximum of 4 self-complementarity to avoid primers to form secondary structures, such as hairpins.

Step 3 – After hitting “Get primers” the program will open a new window in which it will give all the primers (both reverse and forward) inside the chosen parameters above. In some cases the same primer is able to recognize several different variants of the same gene, which is a positive aspect due to the intervariability of the individuals.

Primers were obtained Eurofins Genomics in lyophilized form, then resuspended to obtain the stock solutions to a concentration of 100 µM and further tenfold diluted for the working solutions at 10 µM. The complete list of primers sequences, including the house keeping genes is listed in tables 2, 3 and 4.

Table 2 - Sequence of the Aß-scavengers primers and characteristics

Gene	Accession Number		Primer sequence	Product Size (bp)	Tm (ºc)
IDE	NM_004969.3	Fw	AAGAGGCGACACCATACCCT	243	60,62
		Rv	TATTTTGGAGATCATAGCTCAAGCC		59,0
ACE	NM_000789.3	Fw	GTGTGGAACGAGTATGCCGA	119	60,11
		Rv	GTGCCGTACTTCAGGGTGTG		60,95
GLS	NM_000177.4	Fw	GAAGACCTGGCAACGGATGA	247	60,04
		Rv	AGGGGTCCACAGACCAGTAA		59,81
NEP	NM_000902.3	Fw	GCCTCAGCCGAACCTACAAG	138	60,74
		Rv	CATAAAGCCTCCCCACAGCA		60,03
TTR	NM_000371.3	Fw	GGCATCTCCCCATTCCATGA	181	59,52
		Rv	AATCCCATCCCTCGTCCTTC		58,87
MT2A	NM_005953.3	Fw	AAGAACGCGACTTCCACAAAC	70	59,67
		Rv	AAGGAATATAGCAAACGGTCACG		59,13

Table 3 - Sequence of the circadian rhythm primers and characteristics

Gene	Accession Number		Primer sequence	Product Size (bp)	Tm (ºc)
CLOCK	NM_001267843.1	Fw	GGGCTGAAAGACGACGAGAA	226	60,04
		Rv	GTCGGGATCTTGGTTGGTGT		59,96
BMAL1	NM_001178.5	Fw	TGCCACCAATCCATACACAGA	125	59,37
		Rv	TCTTCCCTCGGTCACATCCT		59,96
PER2	NM_022817.2	Fw	AAGTGAACGAACTGCCCCTG	101	60,54
		Rv	GTTTGACCCGCTTGGACTTC		59,41
PER3	NM_001289862.1	Fw	GCGAATCCCCATCCAGAACT	197	59,82
		Rv	GAGAATGCGCTCAGGTGTCT		60,11
CRY2	NM_021117.3	Fw	CAGGAGAACCACGACGAGAC	242	60,11
		Rv	CGGCAGGAGAGACAACCAAA		60,25

Table 4 - Sequence of the housekeeping genes primers and characteristics

Gene	Accession Number		Primer sequence	Product Size (bp)
PGK1	NM_000291.3	Fw	GAATCACCGACCTCTCTCCC	216
		Rv	AAGGACTACCGACTTGGCTC	
B-Actin	NM_001101.3	Fw	CGCCGCCAGCTCACC	232
		Rv	GCTCGATGGGGTACTTCAGG	

4.2. Primer testing

4.2.1. Polymerase-chain reaction (PCR)

To confirm the expression of IDE, ACE, NEP, GLS, MT2A, TTR, CLOCK, BMAL1, PER2, PER3, and CRY2 genes in human CP it was performed a Polymerase Chain Reaction (PCR). For this purpose, it was used Taq Polymerase (Biotools, B&M Labs S.A.), 50mM $MgCl_2$ Solution (Biotools, B&M Labs S.A.), 10x PCR Reaction Buffer (Roche Diagnostics GmBh) and dNTPS (Roche Diagnostics GmBh), in accordance to the manufacturer's recommendations. The common MIX, using the reagents described above, was prepared in a final volume of 25 µL. The concentration of cDNA for each gene was 1 µg/µL for the positive control, and 0,5 µg/µL for the patients control sample. To the negative control it was added sterile water (from B. Braun Medical SA) instead of cDNA. The primer sequences were added in different concentrations to the common MIX, 100 nM or 200 nM. The samples were incubated on a thermal cycler (PTC-200 Peltier Thermal Cycler, MJ Research) following the steps i) 5 min at 94^0C, ii) 35 cycles with 45 seconds at 94^0C, 30 seconds at optimal primers temperature and 30 seconds at 72^0C, iii) extension step for 10 min at 72^0C.

The amplified products were separated in an agarose gel. The conventional PCR products were previously prepared with DNA loading Buffer 10x (62 % glicerol, 0,42 mg/mL bromophenol blue, 0,42 mg/mL xylene cyanol, 33,3 mM TRIS HCL 1M pH 8, 8,3 mM EDTA 500mM).

This served to confirm that each fragment obtained by the conventional PCR reaction had the expected size by comparison with molecular weight DNA Ladder 100bp (Thermo Fisher Scientifics), and amplified one single product. The gel was visualized under UV transillumination (ChemiDoc XRS, Bio-Rad Laboratories).

4.3. Real-time quantitative PCR

4.3.1. Optimization

The real-time quantitative PCR (RT-qPCR) technique allowed the relative quantification of the Aß-scavengers and circadian rhythm genes. This technique consisted in measuring the amount of cDNA of each gene in question by measuring it after each cycle via fluorescent dyes that produce increasing fluorescent signal in direct proportion to the number of PCR product molecules (amplicons) generated. Then, data collected in the exponential phase of the reaction produce quantitative information on the starting quantity of the amplification

target. The change in fluorescence over the course of the reaction is measured by an instrument that combines thermal cycling with fluorescent dye scanning capability. By plotting fluorescence against the cycle number, the RT-qPCR instrument generates an amplification plot that represents the accumulation of product over the duration of the whole PCR reaction. This technique was able to monitor the progress of the PCR reaction as it occurs in real time, and it was capable to precisely measure the amount of amplicons at each cycle, which allowed highly accurate quantification of the amount of starting materials in samples. The basis of quantification can be explained by stating that if a particular sequence of cDNA is abundant in the sample, amplification is observed in earlier cycles; if the sequence is scarce, amplification is observed in later cycles.

4.3.1.1. Real-time qPCR steps

The presence of three main steps comprises each cycle in a RT-qPCR reaction that could run up about 35 cycles. The denaturation step is a high temperature incubation used to "melt" double-stranded DNA into single strands and loosen the secondary structure in single stranded DNA. The maximum temperature that the DNA polymerase can tolerate is usually 95^0C. Secondly, annealing consists on the hybridization of the complementary sequences, here a proper temperature is used based on the melting temperature (T_m) of the primers, it was used annealing temperatures between 60-64^0C with an annealing time between 30-60 seconds. The higher the annealing temperature, more specific will be the annealing of the primers to the product, and this concept also applies for the annealing time. The annealing temperature and time are used to help the optimization of the reaction, to be more or less specific depending on the results. Lastly, at the extension step the activity of the DNA polymerase is optimal at 70-72^0C, and primer extension occurs at rates of up to 100 bases per second.

4.3.1.2. Real-time qPCR components and groundwork

For the preparation of the RT-qPCR it is necessary to have the right components. SYBR Green master mix (iTaq™ Universal SYBR Green Supermix, Bio-Rad) was used as a dye which contains antibody-mediated hot start iTaq DNA polymerase, dNTPs, $MgCl_2$, SYBR Green I dye, enhancers, stabilizers, and a blend of passive reference dyes. It was used in accordance to the fabricant recommendations. The cDNA template was used in the maximum of 5 µg, excess of template may bring with it higher contaminant levels that can greatly reduce PCR efficiency. The primers were used in concentrations between 100 nM and 200 nM. Templates were pipetted into 96-well clear plates (Hard-Shell® 480 PCR Plates 96-Well, CLR/CLR, Bio-Rad). The reactions were run in a LightCycler 480 Instrument II (Roche Life Science).

4.3.2. Real-time qPCR analysis

For the proper analysis of the RT-qPCR reaction it is necessary to take into account several major terms, including standard curve, its efficiency, slope threshold cycle (Ct), and melting curve.

4.3.2.1. Standard curve

It was used a dilution series of known template concentrations to establish a standard curve to determine the initial starting amount of the target template in experimental samples or for assessing the reaction efficiency. It was optimized a reaction curve for each gene using cDNA of the positive control tissue, which varies along the genes. The concentrations chosen for the standard curve encompass the expected concentration range of the target templates in experimental samples.

4.3.2.2. Slope

The slope of the log-linear phase of the amplification reaction is a measure of reaction efficiency. In order to achieve accurate and reproducible results, reactions should have an efficiency as close to 100 % as possible, corresponding to a slope of -3,32.

4.3.2.3. Efficiency

Theoretically, the efficiency of a PCR reaction should be 100%, meaning the templates doubles after each thermal cycle during exponential amplification. The efficiency can give valuable information about the reaction, including experimental factors, such as the length, secondary structure, and GC content of the amplicon which can influence efficiency. Other factors could influence the efficiency such as handling of the templates and non-correct dilutions of the templates for example. A good reaction should have an efficiency value between 1,9 and 2,1 corresponding to 90% and 110% of efficiency respectively (Figure 5)

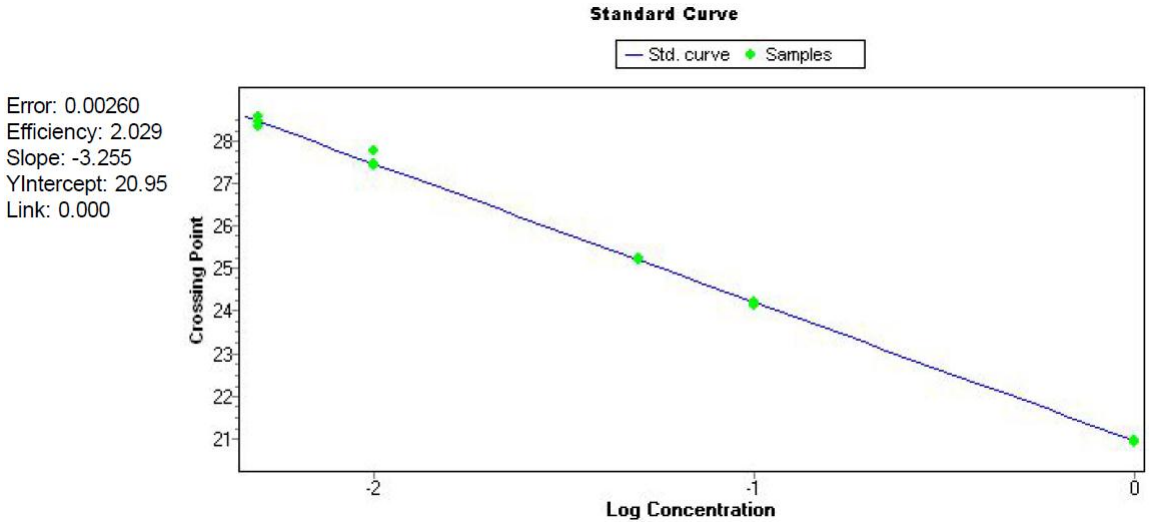

Figure 5 – Example of a standard curve and its respective efficiency and slope (standard curve of MT2A with cortex cDNA).

4.3.2.4. Threshold cycle (Ct)

The threshold cycle (Ct) corresponds to the cycle number at which the fluorescent signal of the reaction crosses the threshold. The latter is the level of the signal that reflects a statistically significant increase over the calculated baseline signal (the signal level during the initial cycles, 3 to 15, in which there is little change in fluorescent signal, it is also considered the "noise" of the reaction). The Ct is used to calculate the initial DNA copy number, due to the fact that Ct value is inversely related to the starting amount of target. For example, samples containing different amounts of target, a sample with twice the starting amount will produce a Ct one cycle earlier than the sample that contained half of the amount of the target prior to amplification.

4.3.2.5. Melting curve (dissociation curve)

A melting curve graphs the change in fluorescence observed when double-stranded DNA (dsDNA) with incorporated dye molecules dissociates, or "melts" into single-stranded DNA (ssDNA) as the temperature of the reaction is raised. When dsDNA bound with the SYBR Green dye is heated, a sudden decrease in fluorescence is detected when the melting point (T_m) is reached, due to dissociation of the DNA strands and subsequent release of the dye. First, the fluorescence is plotted against temperature (Figure 6A) and then the $-\Delta F/\Delta T$ (change in fluorescence/change in temperature) is plotted against temperature to obtain a melting peak, in which is possible to have a view of the melting dynamics (Figure 6B). Analysis of the melting curve after amplification is a simple, straightforward way to check RT-qPCR reactions for primer-dimers presence and to ensure reaction specificity. Every gene product has its own

T_m, thus it has to be the same in the whole reaction, and therefore, any difference in the T_m means that the reaction was not specific.

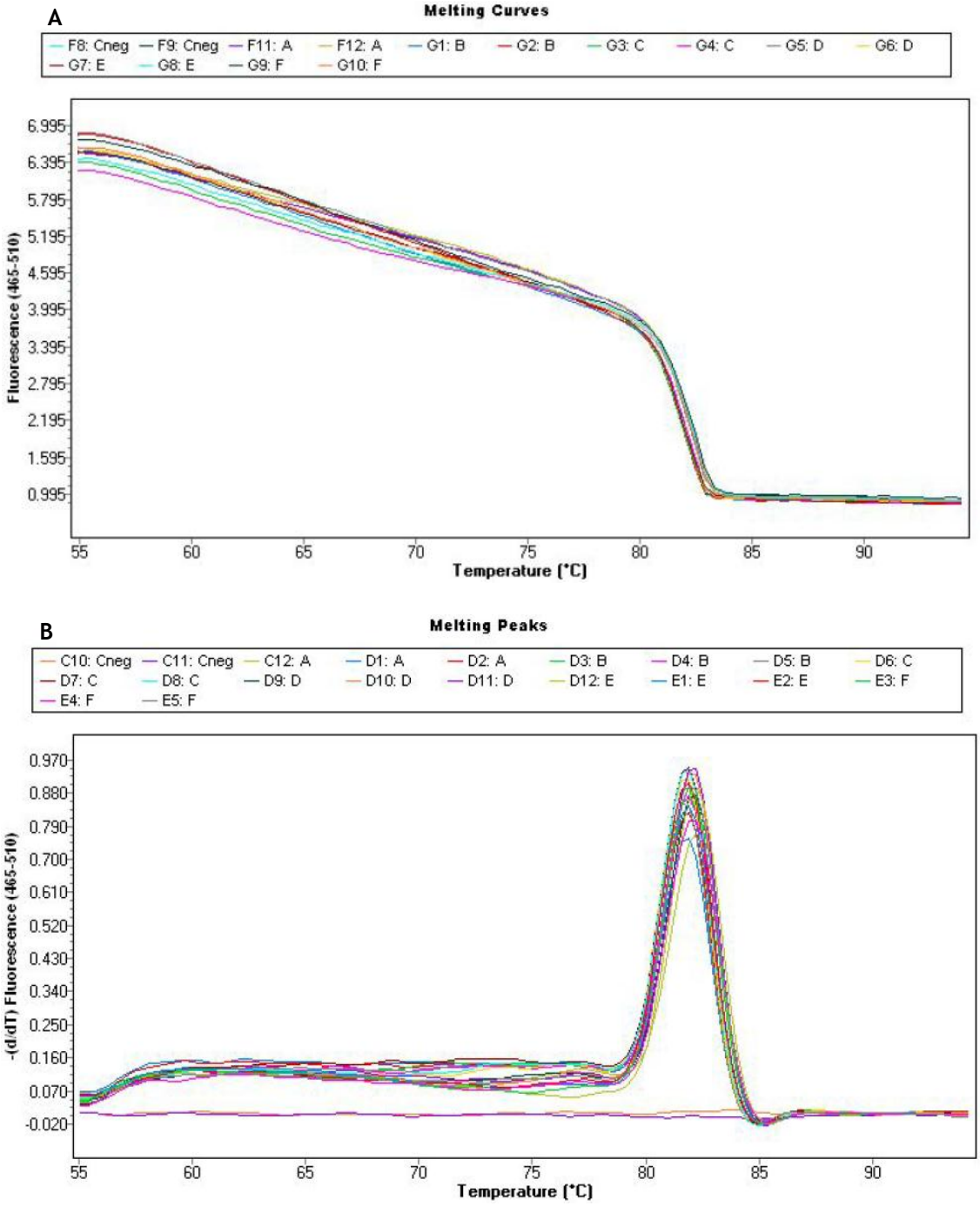

Figure 6 – Example of a (A) melting curve and (B) a melting peak (from RT-qPCR of IDE with cortex cDNA and from RT-qPCR of MME with salivary gland cDNA, respectively).

4.3.2.6. Relative quantification

Relative quantification describes a RT-qPCR experiment in which the expression of a gene of interest in one sample (in this case, the cDNA of CP from AD patients) is compared to expression of the same gene in another sample (in this case, age-matched controls). The results are expressed as fold change, increase or decrease. A housekeeping gene (or normalizer gene) is necessary to use as control for experimental variability in this type of quantification. The housekeeping genes used in this work were ß-actin and phosphoglycerate kinase 1 (PGK1), which were already demonstrated, in previous studies, to be reliable housekeeping genes.

4.3.2.7. Optimized real-time qPCR conditions

For proper relative quantification of genes it is necessary to achieve the optimal reaction conditions for each gene. This includes, primer concentration, annealing temperature and time, and number of cycles, which all of them varies with the gene. In table 5, 6 and 7 are represented the optimized conditions for the Aß-scavengers and circadian rhythm genes, respectively.

Table 5 – Aß-scavengers genes optimized RT-qPCR conditions

Gene	Primers (nM)	Annealing Temp. (^{0}C)	Annealing time (sec.)	cDNA sample
IDE	100	64	30	Hepatic cells
ACE	100	64	60	Salivary gland
GLS	200	60	60	Cortex
NEP	100	64	60	Salivary Gland
TTR	Fw- 100; Rv - 200	62	30	Hepatic Cells
MT2A	200	60	60	Cortex

Table 6 – Circadian rhythm genes optimized RT-qPCR conditions.

Gene	Primers (nM)	Annealing Temp. (^{0}C)	Annealing time (sec.)	cDNA sample
CLOCK	100	64	30	Cortex
BMAL1	200	60	30	Cortex
PER2	200	62	30	Cortex
PER3	100	62	60	Cortex
CRY2	100	64	30	Cortex

The housekeeping genes also needed RT-qPCR reaction optimization, regarding the same terms above described for the Aß-scavengers and circadian rhythm genes. In table 7 are represented the housekeeping genes conditions.

Table 7 – Housekeeping gene PGK1 optimized RT-qPCR conditions.

Gene	Primers (nM)	Annealing Temp. (^{0}C)	Annealing time (sec.)
PGK1	200	60	60
B - Actin	100	62	30

5. Data analysis

RT-qPCR data was analyzed by relative quantification. The PCR signal of the target transcript in the different AD Braak stages was related to age-matched control group. The $2^{-\Delta\Delta Ct}$ method was used for this purpose (Kenneth and Schmittgen, 2001). Firstly, it was necessary to calculate ΔCt (1),

$$\Delta Ct = Ct\ (target\ gene) - Ct\ (housekeeping\ gene \quad (1)$$

Then ΔΔCt was calculated (2),

$$\Delta\Delta Ct = \Delta Ct - \overline{\Delta Ct}\ control\ group \quad (2)$$

Followed by calculus of $2^{-\Delta\Delta Ct}$ giving the fold difference between groups.

6. Statistical analysis

Statistical analysis of Aß-scavengers RT-qPCR results was carried out using GraphPad Prism (Version 6). The experimental data was compared and expressed as mean ± SEM. Comparisons of means between groups was performed using one-way ANOVA followed by Bonferroni's multiple comparison test. Results were considered statistical significant when $p<0.05$.

IV. RESULTS

1. Primer testing

Primer testing was performed by Polymerase Chain Reaction (PCR) using cDNA of tissues where the genes were already described to be expressed in previous studies, as positive control, as well with human choroid plexus cDNA to confirm the expression of the selected genes.

1.1. Aß-scavengers

Angiotensin-converting enzyme (ACE) expression was confirmed by the presence of a single band in the lane zone that corresponds to its molecular weight of 119bp, in agreement with the expected product length (Figure XA), in both human salivary gland, as positive control for this gene (Figure 7A, lane 2), as well as in choroid plexus of a control individual (Figure 7A, lane 1).

Insulin degrading enzyme (IDE) was proven to be expressed in human choroid plexus, with a length of 243bp as it is visible in the respective agarose gel (Figure 7B, lane 1). Previous studies have shown IDE expression in hepatic cells, and therefore HEP G2 (human liver cancer cell line) cDNA was used as positive control (Figure 7B lane 2) (Pivovarova et al., 2015).

Gelsolin (GLS) was found to be expressed in both human cortex as positive control and in choroid plexus, as demonstrated in the agarose gel with the molecular length of 247bp (Figure 7C).

Neprilysin (NEP) expression in human salivary gland, as positive control, and choroid plexus was confirmed by its correspondence with the respective molecular weight of 138bp (Figure 7D).

Transthyretin (TTR) was shown to be highly expressed in the liver, and for this purpose, it was used the same hepatic stellate cells line for positive control as used for IDE gene. IDE expression in both HEP G2 cells and choroid plexus was confirmed by the appearance of a single band corresponding to its length of 181bp (Figure 7E) (Norgren et al., 2014).

Lastly, Metallothionein 2A (MT2A) expression was confirmed in both human cortex, as positive control, and in choroid plexus, with a molecular length of 70bp (Figure 7F).

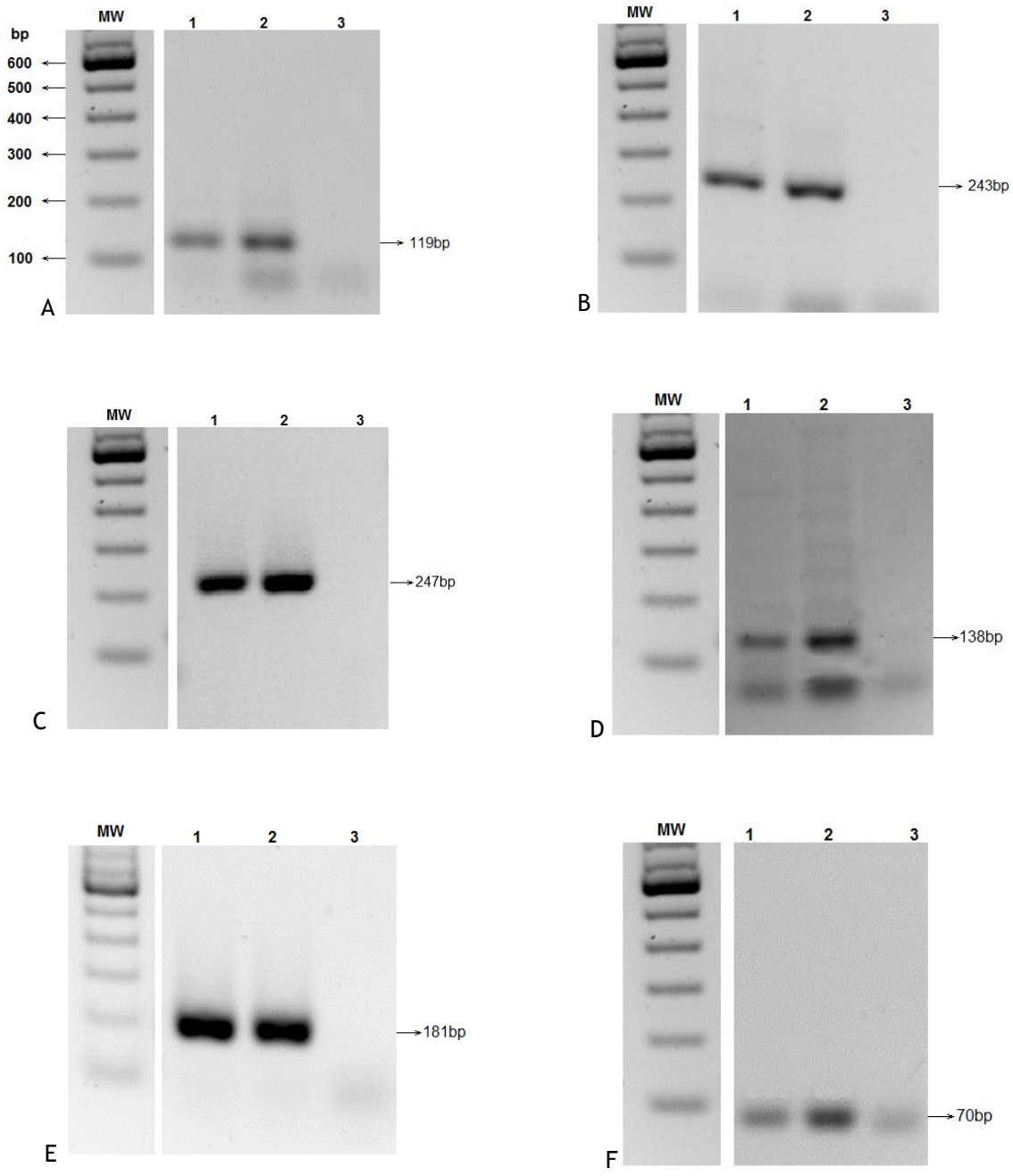

Figure 7 - **Aβ-scavengers genes expression testing**. 1% agarose gels with each respective gene fragment in lanes 1) choroid plexus and 2) positive control with 3) negative control and MW) molecular weight marker, with respective lanes molecular length represented. A) ACE, B) IDE, C) GLS, D) NEP, E) TTR and F) MT2A.

It is worthy to note the presence of a tenuous band below 100bp in some genes and in the negative control corresponding lane, including in Fig. 7 A) ACE, B) IDE, D) NEP, E) TTR and F) MT2A agarose gels. This band corresponds to the existence of primer-dimers. Taking into account that PCR reactions were not optimized in terms of primers concentration, annealing

temperature and time, and due to the fact that some primers have one or more complementarity bases, it is possible to visualize a manifestation of a non-optimized reaction, as primer-dimers formation. The purpose of the primer testing was to confirm if the primers were reliable to the amplification of its corresponding gene, whereas reaction optimization was performed specifically RT-q PCR (section 2).

It was tested for the IDE, TTR, ACE and NEP genes human cortex as positive control. However due to their lack of expression confirmed by electrophoresis, it was necessary to change the positive control tissue to one where its expression was already confirmed before, which is mentioned above.

1.2. Circadian rhythm genes

Primer testing of CLOCK was confirmed by the presence of a band with 226bp of length in agarose gel (Figure 8A) for human cortex and choroid plexus samples.

BMAL1, PER2, PER3 and CRY2 were also confirmed to be expressed in human cortex, as positive control, and choroid plexus with the presence of a band with 125bp in length (Figure 8B), 101bp (Figure 8C), 197bp (Figure 8D) and 242bp (Figure 8E), respectively, by comparison with molecular weight marker.

CRY1 expression was not confirmed in agarose gel, neither with human cortex, choroid plexus, salivary gland nor hepatic stellate cells samples. This suggests that the primers for CRY1 gene might not be able to amplify the gene in question.

As explained before for the Aß-scavengers, the tenuous band below 100bp corresponds to primer dimers.

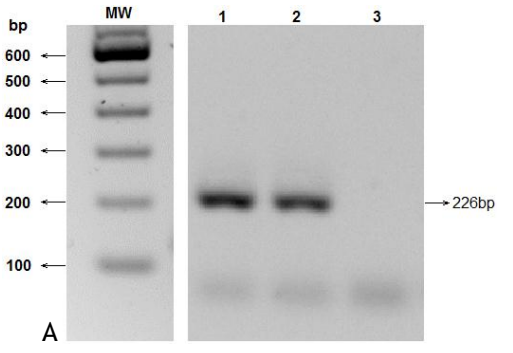
bp
600
500
400
300
200
100
MW
1
2
3
226bp
A

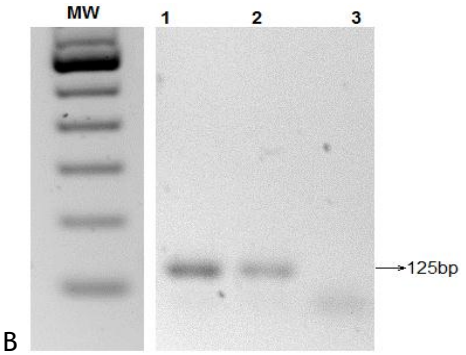
MW
1
2
3
125bp
B

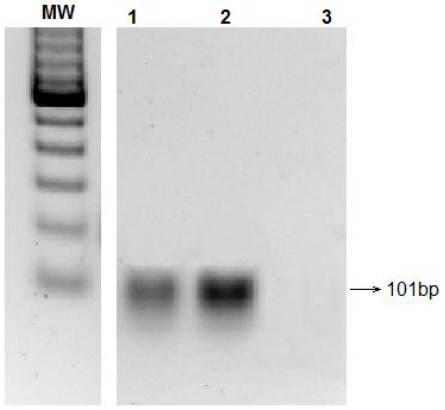
MW
1
2
3
101bp

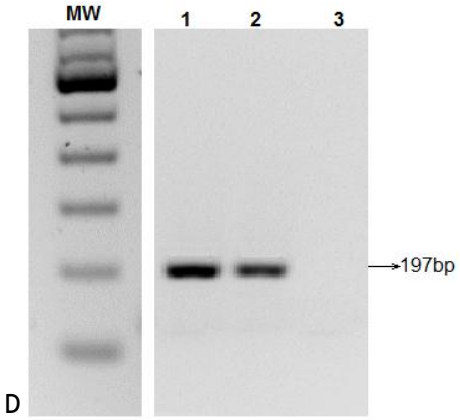
MW
1
2
3
197bp
D

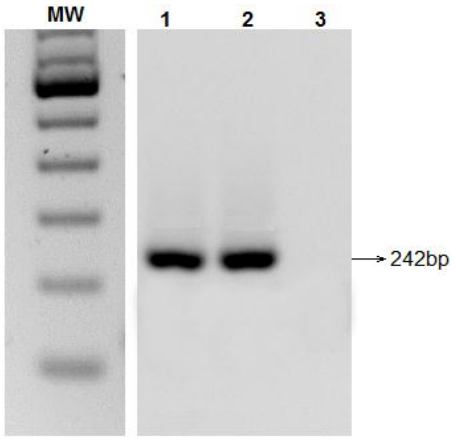
MW
1
2
3
242bp

2. RT-qPCR optimization

All primers for the Aß-scavengers and circadian rhythm genes were optimized for RT-qPCR reactions. The optimization takes into account the right primer concentration, annealing temperature, time of annealing and number of cycles to produce a final standard curve for each gene with an efficiency between 90-110% (1.900-2.100). The standard curve was made up of five to seven dilution series of known template concentrations. The concentrations used for the standard curve encompass the expected concentration range of the target templates in experimental samples. The template used for the construction of the standard curve was cDNA of the positive control, which varies with the genes. The values of the primers optimizations are described in tables 8 and 9, for Aß-scavengers and circadian rhythm, respectively.

Table 8 – RT-qPCR optimized conditions for the circadian rhythm genes.

Gene	cDNA sample	Melting Temperature (^{0}C)	Standard curve dilution range (µg/µL)	Stand. Curve Cts range	Efficiency
IDE	Hepatic Cells	82,6	0.05 - 0.001564	25,1 – 30,6	1,939
ACE	Salivary Gland	82	1 - 0.03125	26,9 – 31,4	2,088
GLS	Cortex	86,2	0.2 - 0.00002	21,8 – 32,3	1,934
NEP	Salivary Gland	82,1	0.125 - 0.00048	27,95 – 35,72	1,954
TTR	Hepatic Cells	88	0.005 - 0.000008	24,9 – 34,5	1,959
MT2A	Cortex	78,5	0.2 - 0.00002	19,87 – 33,2	1,992

Table 9 – RT-qPCR optimized conditions for the circadian rhythm genes.

Gene	cDNA sample	Melting Temperature (^{0}C)	Standard curve dilution range (µg/µL)	Stand. Curve Cts range	Efficiency
CLOCK	Cortex	83.2	0.1 - 0.00078125	26,6 – 33,7	1,942
BMAL1	Cortex	80	0.02 - 0.00015625	26,4 – 33,9	1,973
PER2	Cortex	78,6	0.05 – 0.0001953125	25,1 – 32,9	1,957
PER3	Cortex	81,6	0.05 - 0.000078125	26,6 – 31,7	1,971
CRY2	Cortex	87,6	1 - 0.0015625	27,8 – 33,6	1,963

The normalizer or housekeeping genes PGK1 and ß-actin also needed optimization for the RT-qPCR reactions, regarding the same characteristics for the Aß-scavengers and circadian rhythm genes. The values of RT-qPCR optimization conditions for housekeeping gene PGK1 and ß-actin are described in Table 10.

Table 10 – RT-qPCR optimized conditions for housekeeping genes PGK1 and ß-actin.

Gene	cDNA sample	Melting Temperature (^{0}C)	Standard curve dilution range (µg/µL)	Stand. Curve Cts range	Efficiency
PGK1	Cortex	82,8	0.02 – 0.000078125	26,9 – 35,6	2,036
B - Actin	Cortex	91,2	0,02 – 0,00125	24,5 - 29	1,924

For the optimization of the RT-qPCR reaction conditions, many reactions were performed in order to achieve the best reaction conditions with maximum standard curve efficiency possible, with inexistence of primer-dimers and contaminations with exogenous DNA.

In the process of optimization, some variable parameters suffered changes, including the annealing temperature and time. Whenever a RT-qPCR reaction was not visibly specific, a need to increase the annealing temperature urged, as so diminishing the annealing time. This augmented the reaction specificity to only amplify the gene and anything less. Primer concentration was very important in order to reduce the formation of primer-dimers, if

present. A reduction in primer concentration led to significant improvements in the reaction course.

3. Real-time qPCR relative quantification

3.1. PGK1 housekeeping gene

In order to analyze relative mRNA expression of the TTR, GLS and NEP genes in human choroid plexus a housekeeping gene, PGK1, was needed to normalize the expression levels of these genes. Figure 9 represents the variations of PGK1 of the AD patients.

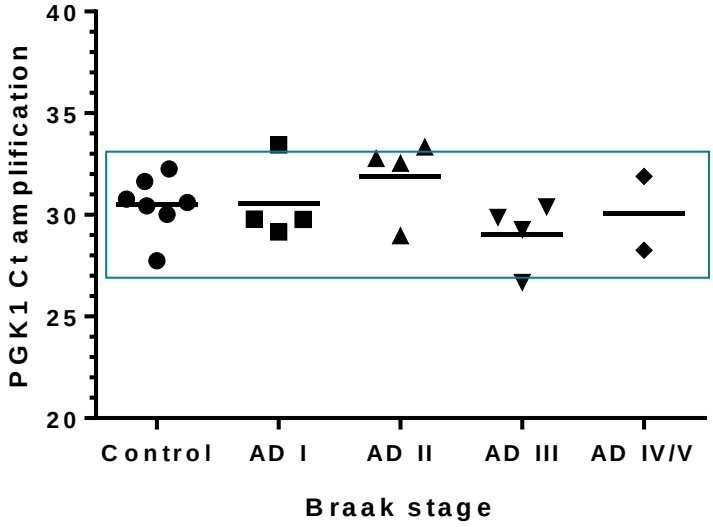

Figure 9 – Graphic representation of the PGK1 Ct amplification in AD patients.

In (Figure 9) the lack of variation of the housekeeping gene PGK1 with the disease stage is shown, what makes PGK1 a proper normalizer gene. There is only a difference of 3 Cts between the samples with more variation, the remaining samples showed close Ct values, suggesting the same level of mRNA expression.

The ß-actin did not have the same behavior as PGK1 in human choroid plexus, its levels of expression among the AD patients' samples had high variations making this housekeeping gene unsuitable to normalize the RT-qPCR reactions.

In an attempt to verify if the Aß-scavengers genes were regulated by Alzheimer's disease in distinct Braak stages of the disease, their expression was compared in the CP of patients with AD by RT-qPCR.

3.2. Transthyretin (TTR)

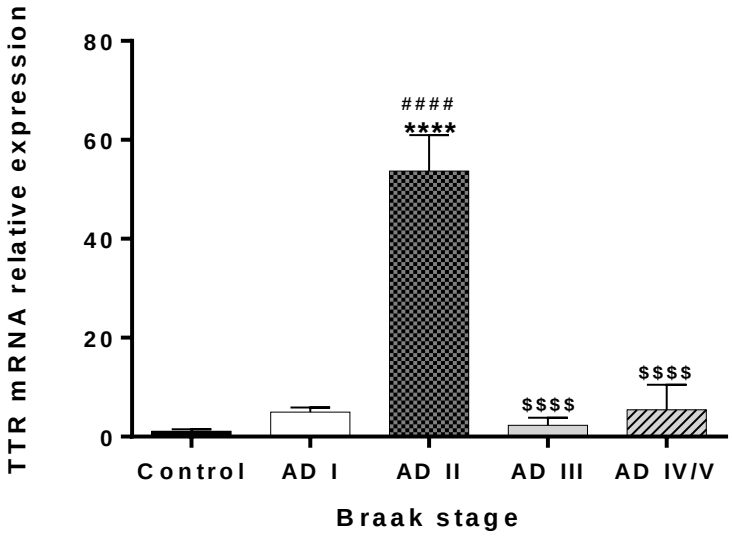

Figure 10 – Comparison of TTR mRNA relative expression between control (Braak stage 0) (n=3), AD Braak stage I (n=4), stage II (n=3), stage III (n=4) and stages IV/V (n=3). Results are expressed as mean ± SEM. **** p< 0.0001, significantly different from control; #### p< 0.0001 significantly different from AD I; $$$$ p< 0.0001, significantly different from AD II.

TTR mRNA levels in CP (Figure 10) displayed a significant difference between the control and Braak stage II (p< 0.0001), showing an upregulation of almost 60 fold. It also showed significant difference between Braak stage I and Braak stage II (p< 0.0001), also between Braak stage II and Braak stages III and IV/V (p< 0.0001). Lack of variation is shown between the control and Braak stages III and IV/V, although between control and Braak stage I, showed a subtle upregulation.

3.3. Gelsolin (GLS)

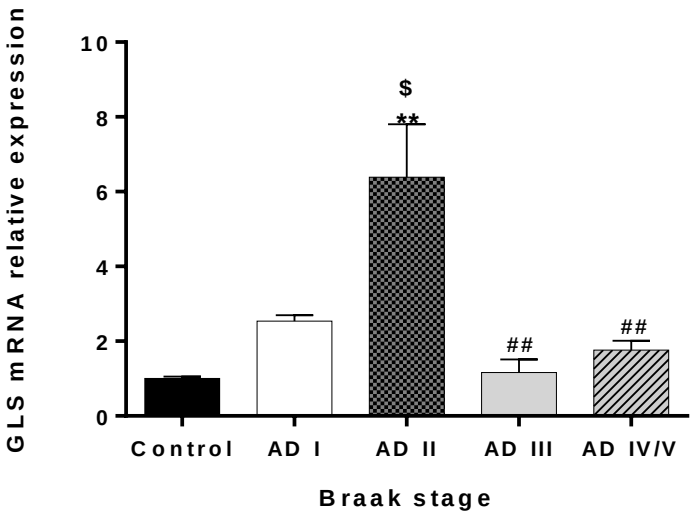

Figure 11 – Comparison of GLS mRNA relative expression between control (Braak stage 0) (n=4), AD Braak stage I (n=5), stage II (n=5), stage III (n=4) and stages IV/V (n=3). Results are expressed as mean ± SEM. ** p< 0.01, significantly different from control; $ p< 0.05, significantly different from AD I; ## p< 0.01, significantly different from AD II.

GLS (Figure 11) levels significantly increased in AD II (p< 0.01) in comparison to the control group. Significant differences in the expression were also seen between AD I and AD II (p< 0.05) and between AD II *vs* AD III (p< 0.01) and AD II *vs* AD IV/V (p< 0.01), where GLS is upregulated in Braak stage AD II in comparison with stages AD III and AD IV/V. It is visible an upregulation of GLS mRNA in the AD II stage in comparison with the remaining ones.

3.4. Neprilysin (NEP)

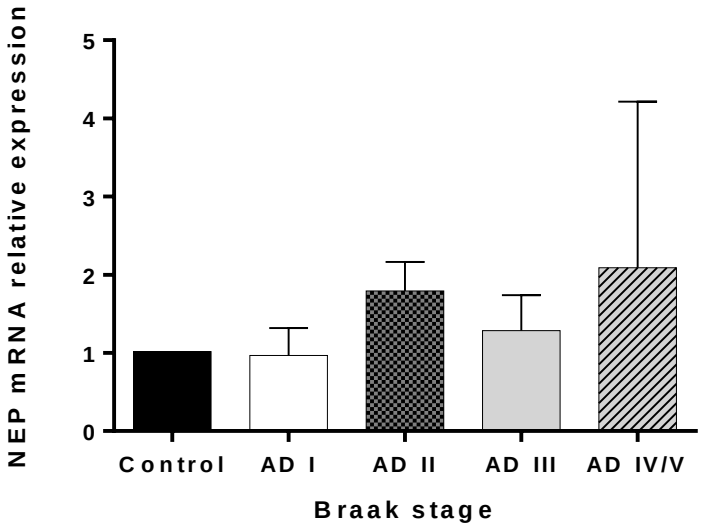

Figure 12 – Comparison of NEP mRNA relative expression between control (Braak stage 0) (n=4), AD Braak stage I (n=6), stage II (n=5), stage III (n=5) and stages IV/V (n=3). Results are expressed as mean ± SEM. ** p< 0.01, * p< 0.05 significantly different from control, Student´s *t*-test.

NEP mRNA expression levels (Figure 12) did not show any significant variation between the Braak stages studied. However, it was noticeable a slight and progressive increase from AD II Braak stage and further stages.

V. DISCUSSION AND CONCLUSIONS

The first and second objectives of this current work, primers design and optimization of RT-qPCR reactions for IDE, NEP, ACE, GLS, TTR and MT2A, CLOCK, BMAL1, PER2, PER3 and CRY2 genes were successfully achieved, being able to amplify specifically the products of interest and also to establish standard curves with high efficiency in a wide range of cycles of amplification.

Regarding the third objective, the results in this current work show, for the first time, the expression of the Aß-scavengers TTR, GLS and NEP in the human CP. Transthyretin (TTR) mRNA expression levels were significantly upregulated between control group and Braak stage II ($p< 0.0001$). TTR is one of the main enzymes secreted by CP where its main function is to transport thyroid hormones, and also possesses high ability to bind Aß peptides in the CSF and, therefore, to decrease the levels of Aß in the brain (Schwarzmen et al., 1996; Ciccone et al., 2016). TTR expression levels also showed statistical difference between Braak stage I and Braak stage II ($p< 0.0001$), and also between the Braak stage II and Braak stages III and IV/V ($p< 0.0001$). TTR results showed a subtle upregulation between control group and Braak stage I, although not statistically different, followed by an abrupt increase in mRNA levels in Braak stage II. The sudden decrease of TTR expression in the stage III, relative to stage II, corresponding to the mild cognitive impairment (MCI) clinical phase, is in agreement with a suggestion of previous authors that in late onset AD patients it occurs a decrease in TTR levels in the CSF resulting in an increase in the Aß plaque formation (Alshehri et al., 2015). The same behavior occurs in stage IV/V, corresponding to an advanced AD stage. Further analysis of TTR protein levels is needed to verify if they are as increased as its mRNA levels.

Gelsolin (GSN) mRNA expression showed statistical significant regulation between age-matched controls and the different stages of AD. The most notorious significant difference is between the Braak stage II and the control group ($p < 0.01$), where GSN showed a six fold upregulation in stage II. The same pattern of expression of TTR is found, a slight increase in expression in stage I, an accentuated increase in stage II followed by an abrupt decrease of expression on stages III and IV/V. In stage II *vs* stage III and stage II *vs* stage IV/V a statistical significant difference is showed ($p < 0.05$). Previous studies demonstrated that GSN is downregulated in advanced stages of AD, although in stages corresponding to clinically silent periods of the disease, as the preclinical stage (Braak stage II), there is no information whatsoever (Chauhuan et al., 1999; Ray et al., 2000). The results in this current study showed that in early stage of AD, there is an upregulation of GSN mRNA expression. In stage II, the disease is far from being fully developed and the CP, still intact, might be able to perform a proper secretion of its enzymes, including TTR and GLS.

Neprilysin (NEP) mRNA expression levels did not show significant difference between the control group and the Braak stages of the disease. However, NEP mRNA expression levels displayed a tendency to increase almost two fold between control group and Braak stage II, also seen in Braak stage IV/V. Previous studies found that NEP protein and activity levels were reduced in the AD brain, specifically in the hippocampus and cortex, where senile plaques

formation and Aß aggregation was present, corresponding to Braak stages IV to VI, an advanced stage of the disease (Baranello et al., 2015; Li et al., 2015). However, NEP mRNA expression results showed a slight alteration in Braak stage III, corresponding to MCI clinical phase of AD in comparison with group control. NEP expression levels in CP of AD patients appears to be upregulated in Braak stage II till Braak stage IV/V, although not possessing statistical difference, but it is displayed with a two fold increase in comparison with the control group. The pattern seen in TTR and GLS expression levels, where there is an obvious upregulation of the genes in Braak stage II, seems to be more subtle in NEP gene levels of expression. However, in NEP it is not followed by an abrupt decrease of expression levels in the following Braak stages. Increased NEP levels in advanced stages of AD may contribute for attenuation of the Aß plaque burden in several brain regions (Li et al., 2015).

Overall, Aß-scavengers mRNA gene levels (TTR and GLS), were upregulated mostly in Braak stage II of the disease. This finding suggests that the CP, in an attempt to compensate the formation of Aß, as a defense mechanism, makes efforts to increase its elimination by, somehow, increasing the expression of enzymes capable of remediating the process, in this case Aß-scavengers. In NEP, this tendency is not as accentuated as in TTR and GLS. It is important to take into account that in AD the CP develops irregularities similar to those related with aging, however very enhanced (Krzyzanowska et al., 2015). Accumulation of Aß in CP epithelial cells, might affect vital function of the CP in AD cases (Vargas et al., 2010), including synthesis, secretion, and transport of proteins or other molecules (Krzyzanowska et al., 2012). In accordance with this information it is expected to verify a general reduction in the levels of CP proteins and/or mRNA levels. The processes involved in the accumulation of Aß in CP might lead to a disruption of protein synthesis in CP and due to the variety of the CP's functions, even a slight modification in the CP can promote extensive effects (Vargas et al., 2010).

The study of circadian rhythm genes in human tissue is extremely difficult to accomplish with reliable results. At the mRNA level, it is important to know exactly when the material was collected during the day. As it is known, the genes that are under the influence of circadian rhythms, a sample collected during the day will be different from the one collecting during the night and *vice-versa* (Thome et al. 2011). For further experiments of circadian rhythmicity of Aß-scavengers, a higher amount of AD patient's CPs with matching times of tissue collection will be necessary.

Further transcriptomic analysis of the remaining Aß-scavengers are needed to verify if the pattern seen in TTR, GLS and NEP, between control and AD Braak stage II where there was an increase in mRNA levels, followed by a decrease of its mRNA levels in more advanced stages of the disease, is also observed for other Aß-scavengers. If the results show the same pattern, it could represent a step closer to ascertain the early events in the pathogenesis of the disease. Together with further experiments regarding the circadian rhythmicity, it could lead to a deep understanding of the disease. As far as it is known, the Aß-scavengers could be,

somehow, correlated with the circadian rhythm clock genes. Future studies should clarify the regulation of these genes in both AD human subjects and AD mouse models for better understanding the circadian clock oscillation and its implication with the Aß-scavengers in an understudied brain region in AD, the CP.

VI. BIBLIOGRAPHY

●Hardy, J. and D. J. Selkoe, (2002). “The amyloid hypothesis of Alzheimer’s disease: progress and problems on the road to therapeutics.” Science 297: 353-356.

● Jack, C. R., D. S. Knopman, W. J. Jagust, L. M. Shaw, P. S. Aisen, M. W. Weiner, R. C. Petersen and J. Q. Trojanowski, (2010). “Hypothetical model of dynamic biomarkers of the Alzheimer’s pathological cascade.” Lancet Neurol. 9: 119-128.

● Morris, J.C., (2005). “Mild cognitive impairment and preclinical Alzheimer’s disease.” Geriatrics Suppl 9-14.

● Lucey, B. P. and R. J. Bateman (2014). "Amyloid-beta diurnal pattern: possible role of sleep in Alzheimer's disease pathogenesis." Neurobiol Aging 35 Suppl 2: S29-34.

● Strooper, B. D., R. Vassar and T. Golde (2010). “The secretases: enzymes with therapeutic potential in Alzheimer disease.” Nat. Rev. Neurol. 6: 99-107.

● Cirrito, J.R., K. A. Yamada, M. B. Finn, R. S. Sloviter, K. R. Bales, P. C. May, D. D. Schoepp, S. M. Paul, S. Mennerick and D. M. Holtzman (2005). “Synaptic activity regulates interstitial fluid amyloid-b levels in vivo.” Neuron 48: 913-922.

● Jarrett, J.T., E. P. Berger and P. T. Lansbury (1993). “The carboxy terminus of the beta-amyloid protein is critical for the seeding of amyloid formation: implications for the pathogenesis of Alzheimer’s disease.” Biochemistry 32: 4693-4697.

● Jack, C.R., D. S. Knopman, W. J. Jagust, L. M. Shaw, P. S. Aisen, M. W. Weiner, R. C. Petersen and J. Q. Trojanowski (2010). “Hypothetical model of dynamic biomarkers of the Alzheimer’s pathological cascade.” Lancet Neurol 9: 119-128.

● Peter K. T. and H. L. Paulson (2012). “A protective mutation” Nature 488: 38-39

● Damkier HH, P. D. Brown, and J. Praetorius, (2013). “Cerebrospinal fluid secretion by the choroid plexus.” Physiol Rev 93: 1847–1892.

● Serot J. M., M. C. Béné, B. Foliguet and G. C: Faure (2000) “Morphological alterations of the choroid plexos in late-onset Alzheimer’s disease” Acta Neuropathol 99: 105-108

● Palha, J. A., N. C. Santos, F. Marques, J. Sousa, J. Bessa, R. Miguelote, N. Sousa and P. Belmonte-de-Abreu (2012). "Do genes and environment meet to regulate cerebrospinal fluid dynamics? Relevance for schizophrenia." Front Cell Neurosci 6: 31.

● Lun, M. P., E. S. Monuki and M. K. Lehtinen (2015). "Development and functions of the choroid plexus-cerebrospinal fluid system." Nat Rev Neurosci 16(8): 445-457.

● Liddelow, S. A. (2015). "Development of the choroid plexus and blood-CSF barrier." Front Neurosci 9: 32.

● Krzyzanowska, A. and E. Carro (2012). "Pathological alteration in the choroid plexus of Alzheimer's disease: implication for new therapy approaches." Front Pharmacol 3: 75.

● Demeestere, D., C. Libert and R. E. Vandenbroucke (2015). "Therapeutic implications of the choroid plexus-cerebrospinal fluid interface in neuropsychiatric disorders." Brain Behav Immun 50: 1-13.

● Baruch, K. and M. Schwartz (2013). "CNS-specific T cells shape brain function via the choroid plexus." Brain Behav Immun 34: 11-16

● Marques, F. and J. C. Sousa (2015). "The choroid plexus is modulated by various peripheral stimuli: implications to diseases of the central nervous system." Front Cell Neurosci 9: 136

● Vargas, T., C. Ugalde, C. Spuch, D. Antequera, M. J. Moran, M. A. Martin, I. Ferrer, F. Bermejo-Pareja and E. Carro (2010). "Abeta accumulation in choroid plexus is associated with mitochondrial-induced apoptosis." Neurobiol Aging 31(9): 1569-1581

● Krzyzanowska A., I. J. Consuegra, C. Pascual, D. Antequera, I. Ferrer and E. Carro (2015) "Expression of Regulatory Proteins in Choroid Plexus Changes in Early Stages of Alzheimer Disease" J Neuropathol Exp Neurol 74(4): 359-369

● Bolos, M., C. Spuch, L. Ordonez-Gutierrez, F. Wandosell, I. Ferrer and E. Carro (2013). "Neurogenic effects of beta-amyloid in the choroid plexus epithelial cells in Alzheimer's disease." Cell Mol Life Sci 70(15): 2787-2797.

● Costa I. C., H. N. Carvalho, L. Fernandes (2013). "Aging, circadian rhythms and depressive disorders: a review" Am J Neurodegener 2(4):228-246

● Musiek, E. S., D. D. Xiong and D. M. Holtzman (2015). "Sleep, circadian rhythms, and the pathogenesis of Alzheimer disease." Exp Mol Med 47: e148.

● Cassone V. M., J. C. Speh, J. P. Card and R. Y. Moore (1988) "Comparative anatomy of the mammalian hypothalamic suprachiasmatic nucleus." J Biol Rhythms 3(1):71-91.

● Golombek D. A. and R. E. Rosenstein (2010). "Physiology of circadian entrainment" Physiol Rev 90:1063–1102.

● Dardente H. and N. Cermakian (2007). "Molecular circadian rhythms in central and peripheral clocks in mammals." Chronobiol Int 24:195–213.

● Thome, J., A. N. Coogan, A. G. Woods, C. C. Darie and F. Hassler (2011). "CLOCK Genes and Circadian Rhythmicity in Alzheimer Disease." J Aging Res 2011: 383091.

● Videnovic, A., A. S. Lazar, R. A. Barker and S. Overeem (2014). "'The clocks that time us' - circadian rhythms in neurodegenerative disorders." Nat Rev Neurol 10(12): 683-693.

● Abe M., E. D. Herzog, S. Yamazaki, M. Straume, H. Tei, Y. Sakaki Y, M. Menaker and G. D. Block (2002) "Circadian rhythms in isolated brain regions." J Neurosci 22: 350–356.

● Marpegan L., A. E. Swanstrom, K. Chung, T. Simon, P. G. Haydon, S. K. Khan, A. C. Liu, E. D Herzog and C. Beaulé (2011) "Circadian regulation of ATP release in astrocytes." J Neurosci 31: 8342–8350.

● Kunieda, T., T. Minamino, T. Katsuno, K. Tateno, J. Nishi, H. Miyauchi, M. Orimo, S. Okada and I. Komuro (2006). "Cellular senescence impairs circadian expression of clock genes in vitro and in vivo." Circ Res 98(4): 532-539.

● Born, J. and I. Wilhelm, (2012). "System consolidation of memory during sleep." Psychol Res 76; 192-203.

● Ju, Y.-E., J.S. McLeland, C. D. Toedebusch, C. Xiong, A. M. Fagan, S. Duntley, J. C. Morris and D. M. Holtzman (2013). "Sleep quality and preclinical Alzheimer's disease." JAMA Neurol 70: 587-593.

● Ju, Y.E., and D.M. Holtzman (2013) "Sleep evaluation by actigraphy for patients with Alzheimer disease—reply." JAMA Neurol 70:1074–1075.

● Roh, J.H., Y. Huang, A. W. Bero, T. Kasten, F. R. Stewart, R. J. Bateman and D. M. Holtzman (2012). "Disruption of the sleep-wake cycle and diurnal fluctuation of amyloid-b in mice with Alzheimer's disease pathology." Sci Transl Med 4(150): 150ra22.

● Roh, J. H., H. Jiang, M. B. Finn, F. R. Stewart, T. E. Mahan, J. R. Cirrito, A. Heda, B. J. Snider, M. Li, M. Yanagisawa, L. de Lecea and D. M. Holtzman (2014). "Potential role of orexin and sleep modulation in the pathogenesis of Alzheimer's disease." J Exp Med 211(13): 2487-2496.

● Ooms, S., S. Overeem, K. Besse, M.O. Rikkert, M. Verbeek, and J.A. Claassen (2014) "Effect of 1 night of total sleep deprivation on cerebrospinal fluid β-amyloid 42 in healthy middle-aged men: a randomized clinical trial." JAMA Neurol 71: 971–977

● Xie, L., H. Kang, Q. Xu, M.J. Chen, Y. Liao, M. Thiyagarajan, J. O'Donnell, D.J. Christensen, C. Nicholson, J.J. Iliff, T. Takano, R. Deane and M. Nedergaard (2013). "Sleep drives metabolite clearance from the adult brain" Science 342: 373–377.

● Evans J. A. and A. J. Davidson (2013). "Health consequences of circadian disruption in humans and animal models." Prog Mol Biol Transl Sci 119: 283–323.

● Bunger M. K., L. D. Wilsbacher, S. M. Moran, C. Clendenin, L. A. Radcliffe, J. B. Hogenesch, M. C. Simon, J. S. Takahashi and C. A. Bradfield (2000). "Mop3 is an essential component of the master circadian pacemaker in mammals." Cell 103: 1009–1017.

● Laposky A., A. Easton, C. Dugovic, J. Walisser, C. Bradfield and F. Turek (2005) "Deletion of the mammalian circadian clock gene BMAL1/Mop3 alters baseline sleep architecture and the response to sleep deprivation" Sleep 2005 28: 395–409.

● Mongrain V., F. La Spada, T. Curie and P. Franken (2011) “Sleep loss reduces the DNA binding of BMAL1, CLOCK, and NPAS2 to specific clock genes in the mouse cerebral cortex” PLoS ONE 6: e26622.

● Wang J. L., A. S. Lim, W. Chiang, W. Hsieh, M. Lo, J. A. Schneider, A. S. Buchman, D. A. Bennett, K. Hu, and C. B. Saper (2015) “Suprachiasmatic Neuron Numbers and Rest-Activity Circadian Rhythms in Older Humans” Ann Neurol 78:317–322

● Van Someren E. J. (2000) “Circadian and sleep disturbances in the elderly.” Exp Gerontol 35: 1229–37.

● Song, H., M. Moon, H. K. Choe, D. H. Han, C. Jang, A. Kim, S. Cho, K. Kim and I. Mook-Jung (2015). "Abeta-induced degradation of BMAL1 and CBP leads to circadian rhythm disruption in Alzheimer's disease." Mol Neurodegener 10: 13.

● Cardone L., J. Hirayama, F. Giordano, T. Tamaru, J. J. Palvimo and P. Sassone-Corsi (2005). “Circadian clock control by SUMOylation of BMAL1” Science 309: 1390–4.

● Volicer L., D. G. Harper and E. G. Stopa (2012) “Severe impairment of circadian rhythm in Alzheimer’s disease” J Nutr Health Aging 16(10): 888-90.

● Cermakian, N., E. W. Lamont, P. Boudreau and D. B. Boivin (2011). "Circadian clock gene expression in brain regions of Alzheimer 's disease patients and control subjects." J Biol Rhythms 26(2): 160-170.

● Miners, J. S., J. C. Palmer, H. Tayler, L. E. Palmer, E. Ashby, P. G. Kehoe and S. Love (2014). "Abeta degradation or cerebral perfusion? Divergent effects of multifunctional enzymes." Front Aging Neurosci 6: 238.

● R. J. Baranello, K. L. Bharani, V. Padmaraju, N. Chopra, D. K. Lahiri, N. H. Greig, M. A. Pappolla and K. Sambamurti1 (2015) “Amyloid-Beta Protein Clearance and Degradation (ABCD) Pathways and their Role in Alzheimer’s Disease” Curr Alzheimer Res 12(1): 32–46.

● Hubin, E., F. Cioffi, J. Rozenski, N. A. van Nuland and K. Broersen (2016). "Characterization of insulin-degrading enzyme-mediated cleavage of Abeta in distinct aggregation states." Biochim_Biophys Acta 1860(6): 1281-1290.

● Pérez A., L. Morelli, J. C. Cresto, and E. M. Castaño (2000) “Degradation of soluble amyloid ß-peptides 1-40, 1-42, and the Dutch variant 1-40Q by insulin degrading enzyme from Alzheimer disease and control brains” Neurochem. Res. 25(2): 247-255

● Kochkina, E. G., S. A. Plesneva, D. S. Vasilev, I. A. Zhuravin, A. J. Turner and N. N. Nalivaeva (2015). "Effects of ageing and experimental diabetes on insulin-degrading enzyme expression in male rat tissues." Biogerontology 16(4): 473-484.

● Tang, W. J. (2016). "Targeting Insulin-Degrading Enzyme to Treat Type 2 Diabetes Mellitus." Trends Endocrinol Metab 27(1): 24-34.

● Nilsson, P., K. Loganathan, M. Sekiguchi, B. Winblad, N. Iwata, T. C. Saido and L. O. Tjernberg (2015). "Loss of neprilysin alters protein expression in the brain of Alzheimer's disease model mice." Proteomics 15(19): 3349-3355.

● Li Y., J. Wang, S. Zhang and Z. Liu (2015) "Neprilysin Gene Transfer: A Promising Therapeutic Approach for Alzheimer's Disease" J. Neurosci. Res. 93: 1325–1329.

● Nalivaeva, N. N., N. D. Belyaev, I. A. Zhuravin and A. J. Turner (2012). "The Alzheimer's amyloid-degrading peptidase, neprilysin: can we control it?" Int J Alzheimers Dis 2012: 383796.

● H. Qiao, R. C. Koya, K. Nakagawa, H. Tanaka, H. Fujita, M. Takimoto and N. Kuzumaki (2004). "Inhibition of Alzheimer's amyloid-ß peptide-induced reduction of mitochondrial membrane potential and neurotoxicity by gelsolin" Neur Agi 26: 849–855.

● Hirko, A. C., E. M. Meyer, M. A. King and J. A. Hughes (2007). "Peripheral transgene expression of plasma gelsolin reduces amyloid in transgenic mouse models of Alzheimer's disease." Mol Ther 15(9): 1623-1629.

● I. Ray, A. Chauhan, J. Wegiel, V. P.S. Chauhan (2000). "Gelsolin inhibits the fibrillization of amyloid beta-protein, and also defibrillizes its preformed fibrils" Brain Research 853: 344-351.

● Chauhan, V. P. S., I. Ray, A. Chauhan, and H. M. Wisniewski (1999). "Binding of Gelsolin, a Secretory Protein, to Amyloid ß-Protein" Bioch and Biophy Res Com 258 (2): 241–246.

● Jochemsen, H. M., W. M. van der Flier, E. L. Ashby, C. E. Teunissen, R. E. Jones, M. P. Wattjes, P. Scheltens, M. I. Geerlings, P. G. Kehoe and M. Muller (2015). "Angiotensin-converting enzyme in cerebrospinal fluid and risk of brain atrophy." J Alzheimers Dis 44(1): 153-162.

● Larmuth, K. M., G. Masuyer, R. G. Douglas, S. L. Schwager, K. R. Acharya and E. D. Sturrock (2016). "Kinetic and structural characterization of amyloid-beta peptide hydrolysis by human angiotensin-1-converting enzyme." FEBS J 283(6): 1060-1076.

● Ciccone, L., S. Nencetti, A. Rossello, E. A. Stura and E. Orlandini (2016). "Synthesis and structural analysis of halogen substituted fibril formation inhibitors of Human Transthyretin (TTR)." J Enzyme Inhib Med Chem: 1-12.

● Alshehri, B., D. G. D'Souza, J. Y. Lee, S. Petratos and S. J. Richardson (2015). "The diversity of mechanisms influenced by transthyretin in neurobiology: development, disease and endocrine disruption." J Neuroendocrinol 27(5): 303-323.

● Alemi, M., C. Gaiteiro, C. A. Ribeiro, L. M. Santos, J. R. Gomes, S. M. Oliveira, P. O. Couraud, B. Weksler, I. Romero, M. J. Saraiva and I. Cardoso (2016). "Transthyretin participates in beta-amyloid transport from the brain to the liver- involvement of the low-density lipoprotein receptor-related protein 1?" Sci Rep 6: 20164.

● Schwarzman, A. L., D. Goldgaber (1996) “Interaction of transthyretin with amyloid beta-protein: binding and inhibition of amyloid formation” Ciba Found. Symp. 199, 146–60;

● Li, X., Y. Song, C. R. Sanders and J. N. Buxbaum (2016). "Transthyretin Suppresses Amyloid-beta Secretion by Interfering with Processing of the Amyloid-beta Protein Precursor." J Alzheimers Dis.

● Chung, R. S., C. Howells, E. D. Eaton, L. Shabala, K. Zovo, P. Palumaa, R. Sillard, A. Woodhouse, W. R. Bennett, S. Ray, J. C. Vickers, A. K. West (2010) “The Native Copper- and Zinc- Binding Protein Metallothionein Blocks Copper-Mediated Aß Aggregation and Toxicity in Rat Cortical Neurons” Plos One 5(8): e12030

● Braak, H. and E. Braak, (1991). “Neuropathological stageing of Alzheimer-related changes.” Acta Neuropathol 82: 239-259.

● Sperling R. and K. Jonson (2013). “Biomarkers of Alzheimer disease: currents and future applications to diagnostic criteria” Continuum 19(2): 325-338.

● Pivovarova, O., C. von Loeffelholz, I. Ilkavets, C. Sticht, S. Zhuk, V. Murahovschi, S. Lukowski, S. Docke, J. Kriebel, T. de las Heras Gala, A. Malashicheva, A. Kostareva, J. F. Lock, M. Stockmann, H. Grallert, N. Gretz, S. Dooley, A. F. Pfeiffer and N. Rudovich (2015). "Modulation of insulin degrading enzyme activity and liver cell proliferation." Cell Cycle 14(14): 2293-2300.

● Richardson, S. J., R. C. Wijayagunaratne, D. G. D'Souza, V. M. Darras and S. L. Van Herck (2015). "Transport of thyroid hormones via the choroid plexus into the brain: the roles of transthyretin and thyroid hormone transmembrane transporters." Front Neurosci 9: 66.

● Harper D. G., E. G. Stopa, V. Kuo-Leblanc, A. C. McKee, K. Asayama, L. Volicer, N. Kowall, A. Satlin (2008) “Dorsomedial SCN neuronal subpopulations subserve different functions in human dementia.” Brain 131:1609–1617.

● Farajnia S., S. Michel, T. Deboer, H. T. Vanderleest, T. Houben, J. H. Rohling, A. Ramkisoensing, R. Yasenkov and J. H. Meijer (2012) “Evidence for neuronal desynchrony in the aged suprachiasmatic nucleus clock.” J Neurosci 32: 5891–5899.

● Teng, F.Y., B.L.Tang (2005) “Widespread gamma-secretase activity in the cell, but do we need it at the mitochondria?” Biochem Biophys Res Commun 328: 1–5.

● Kenneth, J. L., T. D. Schmittgen (2001) “Analysis of relative gene expression data using real-time quantitative PCR and $2^{-\Delta\Delta Ct}$ method” Methods 25: 402-408.

● Alvira-Botero X. and E. Carro (2010) “Clearance of amyloid-ß peptide across the choroid plexus in Alzheimer’s disease.” Curr Aging Sci 3(3): 219-229.